Journal of Inflammation Research

Dovepress
Taylor & Francis Group

Open Access Full Text Article

ORIGINAL RESEARCH

Low-Frequency (1 Hz) Repetitive Trans-Spinal Magnetic Stimulation Attenuates NLRP3-Driven Neuroinflammation and Enhances Motor Recovery in Spinal Cord-Injured Mice

Haiwang Song[1,2], Yuxi Yang[1,2], Lieyu Huang[3], Yumei Li[1,2], Baofei Sun[1,2], Zijiang Yu[1,2], Mudan Zhang[4], Dan Yang[1,2]

[1]Department of Human Anatomy, School of Basic Medicine, Guizhou Medical University, Gui'an New District, People's Republic of China; [2]Key Laboratory of Human Brain Bank for Functions and Diseases of Department of Education of Guizhou Province, College of Basic Medical, Guizhou Medical University, Gui'an New District, People's Republic of China; [3]School of Medical Humanities, Guizhou Medical University, Gui'an New District, People's Republic of China; [4]Department of Radiology, Guizhou Provincial People' s Hospital, Guizhou, People's Republic of China

Correspondence: Mudan Zhang, Department of Radiology, Guizhou Provincial People's HospitalNo, 83 Zhongshan East Road, Nanming District, Guiyang, Guizhou, People's Republic of China, Tel +86 18586855793, Email Zmd0404@163.com; Dan Yang, Department of Human Anatomy, School of Basic Medicine, Guizhou Medical University, NO.6 Ankang Avenue, Gui'an New District, Guizhou, People's Republic of China, Tel +86 18798000353, Email stefanie111@126.com

Purpose: Investigate the effects of repetitive Trans-Spinal Magnetic Stimulation (rTSMS) on motor function recovery and the underlying mechanisms in mice after spinal cord injury.

Methods: rTSMS was applied both in vivo and in vitro, Motor function was evaluated by the Basso Mouse Scale (BMS), grid walking errors, and Motor Evoked Potentials (MEPs). Cell viability, oxidative stress markers, and key proteins including AQP4, Bax, Bcl-2, cleaved caspase-3, inflammatory cytokines, and NLRP3 inflammasome components were analyzed. Retrograde tracing using rAAV/Retro and neuronal markers (NeuN, MAP2, β-III-tubulin) were analyzed by the Microplate Reader, Western Blot, ELISA, and Immunofluorescence (IF).

Results: 1 Hz rTSMS improved motor recovery, reduced lesion size, and enhanced MEPs compared to 20 Hz. It decreased spinal edema and oxidative stress, suppressed apoptosis, and inhibited NLRP3 inflammasome activation in microglia. GFAP was down-regulated, while BDNF and anti-inflammatory cytokines (IL-4, IL-10) increased. Retrograde tracing showed enhanced survival of cortical motor neurons after 1 Hz rTSMS. In vitro, BV2 supernatants after MS reduced pro-inflammatory cytokines and promoted PC12 neuronal survival and maturation.

Conclusion: Specific frequency rTSMS at 1 Hz can inhibit NLRP3 inflammasome expression, reducing inflammation, promoting neuroprotection, and aiding hindlimb recovery after spinal cord injury in mice.

Keywords: spinal cord injury, repetitive trans-spinal magnetic stimulation, microglia, NLRP3 inflammasome, neuroprotection, recovery of motor function

Introduction

Spinal cord injury (SCI) is a highly disabling and irreversible disorder of the central nervous system. Its severe impact significantly reduces patients' quality of life and economic capabilities. Although surgical decompression and methylprednisolone therapy can alleviate some symptoms,[1] the secondary trauma from surgical intervention and the side effects of drug treatment remain major challenges.[2] The treatment of SCI has always been a central focus of neuroscience research, highlighting the urgent need to explore non-invasive, effective, safe, and affordable therapeutic approaches for this condition.

Received: 31 January 2025
Accepted: 28 July 2025
Published: 18 August 2025

Graphical Abstract

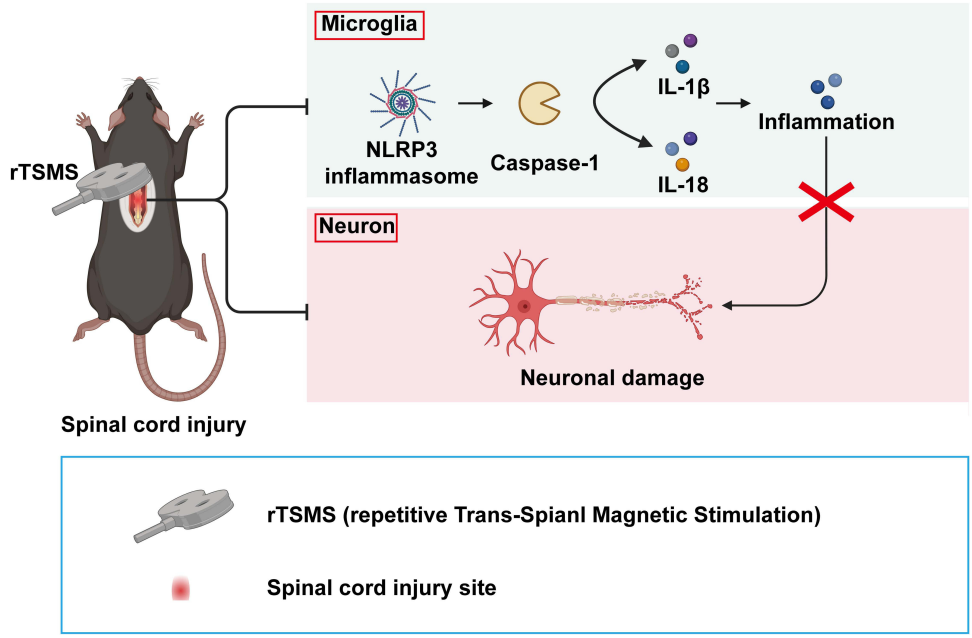

In recent years, repetitive Transcranial Magnetic Stimulation (rTMS) has garnered significant attention in neuroscience due to its non-invasive, safe, adjustable, and quantifiable characteristics.[3] rTMS directly affects cortical neurons by generating a magnetic field, either activating or inhibiting them, thereby altering neural network activity. To investigate the effects of magnetic stimulation at the site of spinal cord injury, termed repetitive Trans-Spinal Magnetic Stimulation (rTSMS), we apply rTMS directly to the spinal cord injury site. This non-invasive stimulation of spinal cord neurons may help regulate inflammatory responses and promote the survival and functional recovery of neurons.[4–6] However, the optimal frequency for therapeutic application remains uncertain. Literature suggests that high-frequency stimulation (≥20 Hz) can improve poststroke cognitive impairment (PSCI) but may also induce seizures.[7] Conversely, low-frequency stimulation (eg, 1 Hz) has been reported to enhance motor function and neuroplasticity in stroke patients.[8,9] Therefore, this study compares the effects of 1 Hz low-frequency and 20 Hz high-frequency rTSMS to explore their impact on motor function recovery in mice after spinal cord injury and investigate the underlying mechanisms.

The NLRP3 inflammasome is the most abundant inflammasome in the central nervous system and a crucial contributor to neuroinflammation in various neurological disorders.[10] It detects intracellular damage signals and activates inflammatory responses, leading to the release of pro-inflammatory cytokines such as IL-1β and IL-18,[11,12] thereby exacerbating neuronal injury and inflammation. Microglia, the primary immune cells involved in the pathological process of spinal cord injury, provide a platform for the activation of the NLRP3 inflammasome.[13] Only microglia express all the necessary components for NLRP3 inflammasome formation (ASC, NLRP3, and CL-Caspase-1).[14] Activation of the NLRP3 inflammasome leads to the release of pro-inflammatory cytokines, worsening neuronal injury and inflammation,[15] which in turn affects neuroprotection and repair processes. Studies have shown that in models such as Alzheimer's disease rodents, Huntington's disease transgenic mice, and brain ischemia-reperfusion models, inhibition of NLRP3 inflammasome activation with MCC950 reduces neuroinflammation, improves cognitive function, and exerts neuroprotective effects.[16–18] However, research on the specific effects of rTSMS on the NLRP3 inflammasome in SCI and its underlying mechanisms remains limited.

Therefore, this study aims to investigate the impact of rTSMS on NLRP3 inflammasome and its mechanisms underlying the recovery of motor function in mice after SCI. By comparing the effects of different frequencies (1 Hz and 20 Hz) of rTSMS on mice, we aim to elucidate whether rTSMS can regulate NLRP3 inflammasome activation to exert neuroprotection and promote motor function recovery. Through this research, we hope to provide new therapeutic strategies and theoretical foundations for the treatment and rehabilitation of spinal cord injury, offering valuable insights for clinical applications and future studies in the field of basic medicine.

Materials and Methods

Primary Experimental Reagents and Instruments

rTSMS Instrument (Shenzhen Yingzhi Technology Co., Ltd., China), Muscle Biopotential Signal Processing System (BIOPAC Systems, Inc., USA), Recording Electrodes and Stimulating Electrodes (Suzhou Lepus Electronics Co., Ltd., China), Cryostat (MEV Technology Co., Ltd, Germany), Laser Scanning Confocal Microscope (Olympus Corporation, Japan), AAV2/Retro virus (pAAV-hSyn-EGFP-3xFLAG-WPRE (Obio Technology (Shanghai) Corp., Ltd., China), RIPA Buffer, Dapi (Beijing Solibao Technology Co., Ltd., China), PMSF, BCA Protein Assay Kit (Shanghai Beyotime Biotechnology Co., Ltd., China), SDS-PAGE Electrophoresis System (Bio-Rad Laboratories, Inc., USA), MCC950 (Sigma-Aldrich, USA), Protein Marker (BioScience Co., Ltd., Shanghai, China), Rabbit Anti-AQP4, Rabbit Anti-BAX, Rabbit Anti-Bcl-2, Rabbit Anti-Cleaved-Caspase-3 (CL-Caspase-3), Rabbit Anti- ASC, Rabbit Anti-Cleaved-Caspase-1 (CL-Caspase-1), Rabbit Anti-IL-1β, Rabbit Anti-IL-18 (Shenyang Wanlei Biotechnology Co., Ltd., China), Rabbit Anti-TNF-α, Rabbit Anti-IFN-γ, Rabbit Anti-IL-4, Rabbit Anti-IL-10 (Shenyang Wanlei Biotechnology Co., Ltd., China), Rabbit Anti-Iba-1, Mouse Anti-NLRP3, 488-labeled Goat Anti-Rabbit IgG, 488-labeled Goat Anti-Mouse IgG, 555-labeled Goat Anti-Rabbit IgG (Abcam (Shanghai) Trading Co., Ltd., UK), Rabbit Anti-IL-6, Rabbit Anti-NeuN, Rabbit Anti-BDNF, Rabbit Anti-GFAP (Boster Biological Technology Co., Ltd., China), Rabbit Anti-MAP2, HRP-conjugated Affinipure Goat Anti-Rabbit IgG, Rabbit Anti-β-actin (Wuhan Proteintech Biotechnology Co., Ltd., China), Rabbit Anti-β-III-tubulin (Jiangsu Affinity Biotechnology Research Center Co., Ltd)., BV2 and PC12 cells (Wuhan Pricella Biotechnology Co., Ltd)., Dulbecco's Modified Eagle Medium High Glucose (4.5 g/L)(Thermo Fisher Scientific Inc)., Fetal Bovine Serum (Zhejiang Tianhang Biotechnology Co., Ltd)., Penicillin-Streptomycin (Suzhou New cell and Molecular Biotech Co., Ltd)., TNF-α, IL-1β, IL-6, TGF-β1, IL-4 and IL-10 ELISA kit (Wuhan Elabscience Biotechnology Co., Ltd)., CCK8 (ApexBio Technology, LLC), LDH (Shanghai Beyotime Biotechnology Co., Ltd).

Experimental Animals

In this study, we used 12-week-old C57BL/6J mice (25 ± 2 g) from the Experimental Animal Center of Guizhou Medical University (Guizhou, China), with an equal male-to-female ratio. The mice were certified under license SCXK (Qian) 2023–0002, and all procedures were approved by the Ethics Committee of Guizhou Medical University (Approval No. 2100034), following the "Guidelines for Ethical Review of Animal Welfare in Experiments" (GB/T 35892–2018). Animal handling, surgery, and all experimental operations strictly adhered to the "Regulations on the Administration of Experimental Animals" issued by China's National Science and Technology Commission, as well as specific guidelines for animal care and management set by the Ethics Committee.

Spinal Cord Injury Model Establishment

Mice were anesthetized by intraperitoneal injection of 1% sodium pentobarbital (0.5 mg/10 g body weight). The back muscles and vertebrae were dissected along the midline. Following T9 laminectomy, the lateral edges of the T9 articular processes were carefully nibbled away using fine forceps to fully expose the spinal cord. A microvascular clip (with a 0.2 mm tip and a tension of 30 g) was used to clip the spinal cord for 10s post T9 laminectomy.[9] During this period, gradual narrowing of the posterior spinal vein was observed, accompanied by twisting or twitching of the hind limbs, curling of the tail, and eventual loss of autonomous movement in the hind limbs and tail at approximately 30 seconds. The incision was rinsed with physiological saline, and muscles, fascia, and skin were sequentially sutured. The wound was then disinfected with iodine solution. Postoperatively, mice were housed individually in a temperature-controlled

animal room with free access to food and water. Bladder emptying was performed manually twice daily (morning and evening at 9:00) until spontaneous urination recovery. Care was taken to keep the urethral orifice dry, disinfecting it daily, and administering intramuscular penicillin (0.1 ml) as needed to prevent infection. Mice in the Sham group underwent the same procedure except for spinal cord compression.

Cell Culture and Co-Culture System Establishment

In this cell experiment, BV2 cell line and PC12 cell line were used as substitutes for microglia and neurons, respectively. BV2 cells were seeded at a density of 1×10^5 cells per well in a 6-well plate, with each well supplemented with 3 mL of complete culture medium (DMEM containing 10% FBS and 1% penicillin/streptomycin). The cells were cultured at 37° C in a 5% CO_2 cell culture incubator. During the cultivation process, change the culture medium every two days. Passage the cells when they reach 80%-90% confluence. BV2 and PC12 cells were treated with 1 μg/mL of LPS to establish the injury model.[19] In addition, to study the relationship between Magnetic Stimulation (MS) and MCC950, following previous research findings, we used 10 μM MCC950 after inducing BV2 cell damage with LPS to observe its interaction with the MS group.[20] In this experiment, the supernatants from BV2 cells treated with MS and MCC950 are respectively named MS BV2-CM and MCC950 BV2-CM. BV2 CM is collected, centrifuged at 5000×g for 5 minutes, and the supernatant is collected for culturing PC12 cells to establish a co-culture system.

Establishment of rTSMS System

Application in animals: Early after spinal cord injury (1 day post-injury). A circular magnetic stimulation coil (Pulsed Magnetic Field Stimulator, YingzhiTech, Shenzhen, China) was gently positioned on the skin surface above the spinal cord injury site, with the coil (inner diameter: 25 mm, outer diameter: 120 mm) center precisely aligned over the lesion epicenter to ensure focal, consistent stimulation.[21,22] The coil was fixed in place using a cantilever arm to maintain consistent positioning throughout the intervention. Stimulation parameters were set using QuickStim V3.2.3 software. The absolute magnetic intensity was set at 1 Tesla (peak intensity: 7 Tesla), corresponding to 25% of the resting motor threshold (RMT). Two stimulation frequencies (1 Hz and 20 Hz) were used. Each session consisted of 40 trains, each delivering 10 biphasic pulses over 10 seconds, with a 5-second inter-train interval, totaling 400 pulses per session.[9] Stimulation sessions were conducted at 9:00 AM after bladder emptying, five days per week with two rest days, for 21 days. Application in cells: The culture dishes will be placed 1 cm away from the center of the cross of the circular coil. According to previous reports,[23] BV2 cells are subjected to Magnetic Stimulation (MS) with a stimulation intensity of 1 Tesla, a frequency of 1 Hz (inter-train interval 26 s), and continuous stimulation for 4 seconds per session. This MS treatment is administered once daily, lasting 10 minutes each time, over 2 days, totaling 2 sessions.

Experimental Animal Grouping

This study involved a total of 150 mice, randomly allocated into the following groups: ① Sham operation group (Sham group): Mice undergoing Sham surgery with removal of vertebral lamina without spinal cord injury. ② Spinal cord injury group (SCI group): Mice undergoing spinal cord injury through laminectomy followed by spinal cord compression without rTSMS intervention. ③ SCI+ 1 Hz rTSMS group (1 Hz group): Mice in the SCI group receiving rTSMS at 1 Hz frequency after spinal cord injury. ④ SCI+ 20 Hz rTSMS group (20 Hz group): Mice in the SCI group receiving rTSMS at 20 Hz frequency after spinal cord injury. ⑤ SCI+ MCC950 group (MCC950 group): Mice in the SCI group receiving MCC950 intervention after spinal cord injury. As reported in previous studies,[24,25] MCC950, an NLRP3 inhibitor, was dissolved in 0.1 M phosphate-buffered saline (PBS) (pH 7.4) at a final concentration of 5 mg/mL and administered via intraperitoneal injection at 1 and 3 hours post spinal cord injury (100 μL, 0.5 mg/10 g). Mice with a Basso Mouse Scale (BMS) score of ≤ 0 after spinal cord injury were selected for subsequent experiments. In BV2 cells, they are divided into groups, ① Con group (LPS^- and MS^- and $MCC950^-$), ② LPS group (LPS^+ and MS^- and $MCC950^-$), ③ MS group ($LPS^+$and MS^+ and $MCC950^-$), ④ MCC950 group ($LPS^+$and MS^- and $MCC950^+$). In PC12 cells, they are divided into groups, ① Con group (LPS^- and MS BV2-CM^- and MCC950 BV2-CM^-), ② LPS group ($LPS^+$and MS BV2-CM^- and MCC950 BV2-CM^-), ③ MS BV2-CM group (LPS^+ and MS BV2-$CM^+$and MCC950 BV2-CM^-), ④ MCC950 BV2-CM group (LPS^+ andMS BV2-CM^- and MCC950 BV2-CM^+).

Behavioral Assessments

Basso Mouse Scale (BMS) Score: BMS score is used to assess the recovery of hind limb motor function in mice after SCI. The evaluations were conducted at 21:00 each night after manually expressing the bladder of the mice. Each group of mice was assessed one day before surgery and at 1 d, 3 d, 7 d, 14 d, and 21 d after SCI. Mice were placed in a 100 cm × 100 cm organic glass box and allowed to freely move for 10 minutes to acclimate to the environment. Subsequently, the motor function of each group of mice was recorded, maintaining a quiet laboratory environment to avoid disturbing the mice. The hind limb motor recovery of the mice was assessed according to detailed BMS scoring criteria and subjected to statistical analysis.

Grid walk test: In the grid walk test, a 50 cm × 50 cm grid runway was used, with each small grid forming a 15 mm×15 mm hole. Prior to the experiment, mice were allowed to freely explore the grid runway for 5 minutes. An error was recorded when a mouse's hind paws and heels completely fell into a square. For analysis, at least 2 minutes of continuous walking time is required. Two researchers recorded the total number of hind limb steps and errors, and calculated the average error rate.

Experimenters assessing BMS scores and Grid walk test were blinded to treatment groups using coded videos. Randomization was stratified by baseline weight and sex using a computer-generated sequence.

Motor Evoked Potentials (MEPs)

MEPs Amplitude in SCI models is associated positively with Preserved Tissue at the SCI Site.[26] On the 21st day post-spinal cord injury, mice were anesthetized with 1% sodium pentobarbital (0.5 mg/10 g) via intraperitoneal injection. Recording electrodes were positioned with the positive and negative poles inserted into different locations of the ipsilateral gastrocnemius muscle, while the ground electrode was inserted subcutaneously at the neck. The stimulating electrode was placed 5 mm above the SCI site to elicit MEPs and record their amplitudes. Stimulation parameters were set at 200 mV voltage and 1 Hz frequency. MEPs were observed and recorded using electrophysiological recording software for each group of mice.

Spinal Cord Water Content Measurement

On day 21 after SCI, mice were anesthetized with 1% pentobarbital sodium (0.5 mg/10 g). The T9 spinal cord segment, 0.5 cm in length, was quickly dissected out, weighed for wet weight, and then dried in an 80°C oven until a constant weight was achieved over 24 hours. The degree of edema in this segment was calculated as (wet weight - dry weight) / wet weight × 100%.

Western Blot

On day 21 after SCI, mice were anesthetized with 1% pentobarbital sodium (0.5 mg/10 g body weight). A 0.5 cm segment of spinal cord tissue adjacent to the injury site was dissected out and placed into a grinding tube. 1 mL of protease inhibitor (RIPA buffer: PMSF = 100:1) was added, and the tissue was homogenized to a uniform consistency. In cells: Discard the culture medium, wash the cells three times with PBS, and lyse them on ice with protease inhibitor for 30 minutes. The supernatant was collected after centrifugation and mixed with Loading Buffer, followed by denaturation at 100°C in a water bath for 5 minutes to denature the proteins. Protein quantification was performed using a BCA assay kit. The proteins from each group were loaded onto a 10% SDS-PAGE gel for electrophoresis, followed by transfer onto a polyvinylidene difluoride (PVDF) membrane. Subsequently, the membrane was incubated with specific primary antibodies followed by secondary antibodies. Protein bands on the PVDF membrane were visualized using ECL substrate, and quantitative analysis of band intensities was performed using ImageJ software. Specific antibody dilutions used were as follows: Bax (1:1000), Bcl-2 (1:1000), Cleaved-Caspase-3 (CL-Caspase-3) (1:1000), AQP4 (1:2000), NLRP3 (1:1000), ASC (1:500), Cleaved-Caspase-1 (CL-Caspase-1) (1:1500), IL-1β (1:1000), IL-18 (1:1500), GFAP (1:3000), BDNF (1:2000), TNF-α (1:1000), IFN-γ (1:2000), IL-6 (1:3000), IL-4 (1:3000), IL-10 (1:2000), β-actin (1:5000), and HRP-conjugated Affinipure Goat Anti-Rabbit IgG (1:10,000).

Immunofluorescence

On day 21 after SCI, mice were anesthetized with 1% pentobarbital sodium (0.5 mg/10 g body weight) and perfused with PBS followed by PFA fixation. Tissue embedding was performed after dehydration through 20% and 30% sucrose gradients, followed by freezing and sectioning using a cryostat at a thickness of 30 μm. In cells: Fix cells with 4% paraformaldehyde at room temperature for 30 minutes. Sections and cells were then incubated in 0.1% Triton X-100/ 0.1M TBS containing 5% bovine serum albumin for 60 minutes. Subsequently, primary antibodies were applied and incubated for 12 hours, followed by incubation with corresponding secondary antibodies (all at a 1:500 dilution) at room temperature for 2 hours, and then stained with DAPI (1:500) for 15 minutes at room temperature. Sections were washed three times with PBS and mounted using anti-fade mounting medium. Specific antibody dilutions used were: Iba-1 (1:250), NLRP3 (1:200), GFAP (1:200), NeuN (1:250), MAP2 (1:200), β-III- tubulin (1:200).

rAAV/Retro-Mediated Retrograde Labeling of Cortical Motor Neurons

Retrograde labeling of cortical motor neurons projecting to the spinal cord was achieved using a rAAV/Retro virus (pAAV-hSyn-EGFP-3xFLAG-WPRE; viral titer: 2.43×10^{13} vg/mL). To detect potential leakage during injection, we premixed 1 μL of Fast Green dye with 5 μL of viral solution. After establishing a SCI model at the T9 level, a Hamilton microsyringe was used to inject the virus into the spinal cord. The injection was performed at the dorsal side of the T10 spinal segment with a needle insertion depth of approximately 1.5 mm, targeting the ventral horn region. The needle was kept in place for 3 minutes to minimize backflow. Subsequently, 2 μL of viral solution was slowly injected into the spinal cord, targeting the bilateral ventral horns at the same spinal segment. Following injection, the needle was left in place for an additional 5 minutes before being slowly withdrawn. After injection, the dura mater, muscle layers, and skin were sutured in sequence. Mice were then placed in a warming chamber until fully recovered from anesthesia. At 21 days post-injection, brain tissues were collected from each group of mice and cryosectioned. The sections were stained using immunofluorescence and subsequently imaged with a confocal fluorescence microscope.

CCK8 and LDH

CCK8: According to the CCK8 protocol, inoculate cell suspension (100 μL/well) into a 96-well plate. Pre-incubate in a CO_2 incubator (37°C, 5% CO_2) for 24 hours, then add 10 μL of CCK-8 solution to each well. Incubate in the incubator for 2 hours. Measure absorbance at 450 nm using a microplate reader. LDH: According to the LDH kit protocol, collect cell culture supernatant, centrifuge at 1000×g for 5 minutes, take 120 μL of supernatant for testing, add 60 μL of LDH working solution and mix well, incubate at room temperature in the dark for 30 minutes, then measure absorbance at 450 nm wavelength.

ELISA

According to the ELISA kit protocol, collect cell culture supernatant, centrifuge at 1000×g for 20 minutes, and use the supernatant for testing. Add 100 μL of biotinylated antibody working solution to each sample, and incubate at 37°C for 60 minutes. Then add 100 μL of HRP enzyme conjugate working solution, and incubate at 37°C for 30 minutes. Add 90 μL of substrate solution, and incubate at 37°C for 15 minutes. Finally, add 50 μL of stop solution, and read absorbance at 450 nm wavelength.

Statistical Analysis

Statistical analysis was performed using SPSS 26.0 and GraphPad Prism 8.0. Data are presented as mean ± standard deviation (mean ± SD). One-way ANOVA followed by Tukey's post hoc test was used for multi-group comparisons. For comparisons between two groups, unpaired two-tailed Student's *t*-test was applied. Statistical significance was set at $P < 0.05$. Group differences were considered significant based on post hoc test results.

Results

1 Hz rTSMS Improves Motor Function in SCI

Locomotor performance was evaluated using the Basso Mouse Scale (BMS) and grid walk test at multiple time points post-injury. Mice in the SCI group displayed pronounced deficits, with persistently low BMS scores and high error rates on the grid test. In contrast, 1 Hz rTSMS treatment led to a marked improvement in both parameters, especially evident at 21 days post-injury. Notably, mice in the 1 Hz group exhibited significantly better recovery than those in the 20 Hz group as shown by BMS ($P = 0.0025$) and grid walk test ($P = 0.0042$). (Figure 1A and B). The gross images of SCI and the statistical results of injury area for each group were assessed at 21 days post-injury, with the injury area measured in square millimeters (mm^2). The Sham group exhibited no injury area, indicating a normal physiological state. The SCI group displayed the largest injury area, reflecting the severity of the injury. Compared to the SCI group, the injury areas were smaller, particularly in the 1 Hz ($P = 0.0039$) and 20 Hz groups ($P = 0.0211$). (Figure 1C and D). These results indicate that low-frequency stimulation exerts a stronger neuroprotective effect on spinal cord tissue integrity and lesion containment. To assess electrophysiological outcomes, motor evoked potentials (MEPs) were recorded in each group.

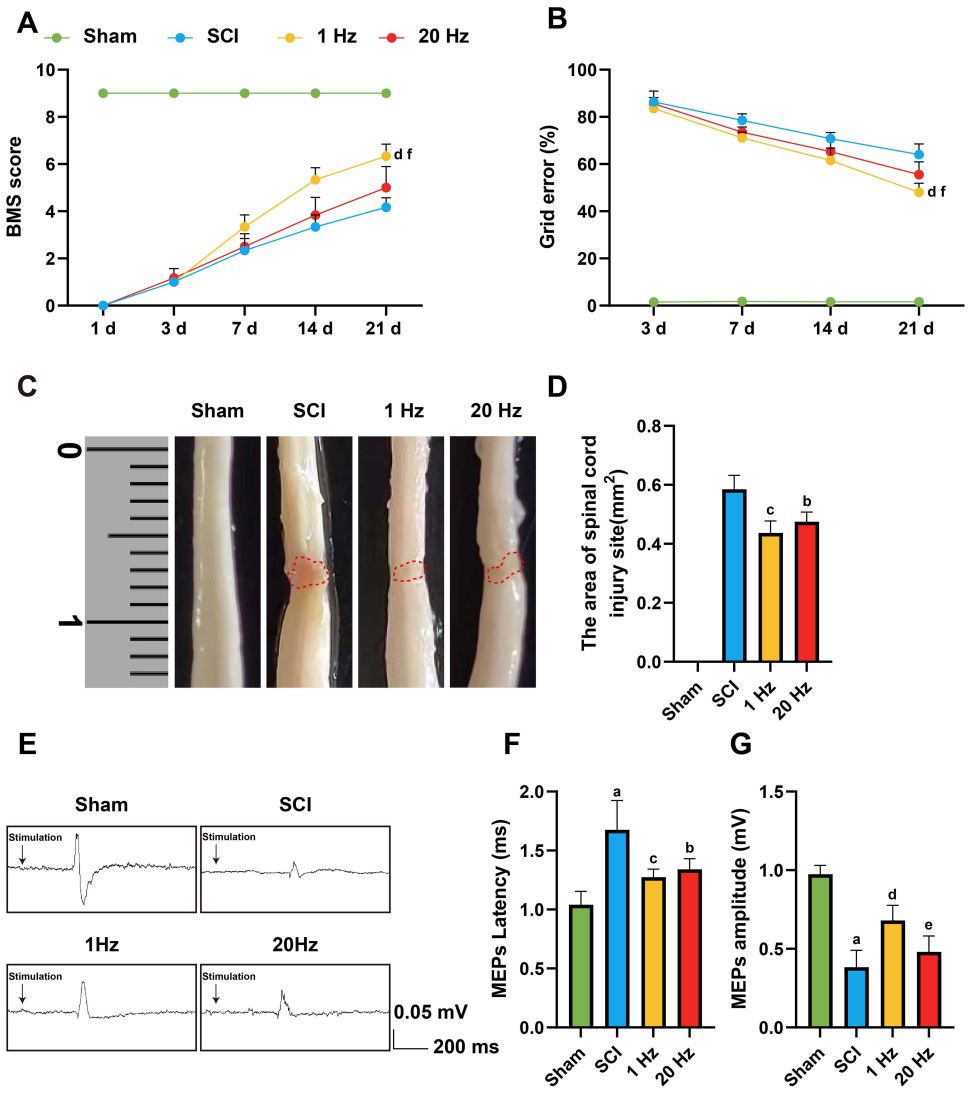

Figure 1 1Hz rTSMS promotes motor function recovery after spinal cord injury. (**A** and **B**) Motor function was assessed using BMS scores and Grid walk test at different time points for Sham, SCI, 1 Hz, and 20 Hz groups, n=8. (**C** and **D**) Images of the spinal cord injury from each group at 21 days after SCI and statistical analysis, n=3. (**E**) Representative recordings and analysis of MEPs in different groups at day 21 after SCI. (**F** and **G**) Quantification of MEPs latency and amplitude. n=5. Scale bar: 0.05 mV/200 ms. $^{a}P<0.001$, vs Sham group. $^{b}P<0.05$, $^{c}P<0.01$, $^{d}P<0.001$, vs SCI group. $^{e}P<0.05$, $^{f}P<0.01$, vs 1 Hz group. The data are expressed as the mean ± SD.

https://doi.org/10.2147/JIR.S516006

SCI mice exhibited significantly prolonged MEP latency and reduced amplitude, reflecting impaired corticospinal conduction. These abnormalities were significantly ameliorated by 1 Hz rTSMS (Latency, P =0.0117; Amplitude, P =0.0006) and 20 Hz rTSMS (Latency, P =0.0089), which restored both latency and amplitude closer to sham levels (P =0.0117) (Figure 1E–G). The improved MEP characteristics suggest enhanced axonal excitability and synaptic transmission in the spinal circuitry following low-frequency stimulation. Collectively, these findings demonstrate that 1 Hz rTSMS facilitates functional and structural recovery following SCI. Compared with 20 Hz stimulation, 1 Hz not only improved behavioral outcomes and reduced lesion size but also enhanced electrophysiological connectivity, supporting its potential as an optimized non-invasive neuromodulation strategy for spinal cord injury repair. These results provide strong evidence for the therapeutic advantage of 1 Hz rTSMS in restoring locomotor function and promoting neural repair in the chronic phase of SCI.

1 Hz rTSMS Mitigates Apoptosis, Spinal Edema, and Oxidative Stress After SCI

After SCI, increased water content at the injury site causes edema. Aquaporin 4 (AQP4), a major member of the water channel protein family in the central nervous system, plays an indispensable role in the development of edema.[27] Therefore, we assessed the levels of AQP4 protein and spinal cord water content. The results indicated that the Sham group exhibited the lowest spinal cord water content and AQP4 protein expression, while the SCI group reached a peak (P = 0.001). After rTSMS intervention, both spinal cord water content and AQP4 protein expression were lower than in the SCI group, with 1 Hz proving more effective than 20 Hz (P = 0.042), as shown in Figure 2A–C.

Apoptosis is a significant cell death mechanism during SCI, involving various cell types such as neurons and microglia.[28] We detected the expression of apoptosis-related proteins BAX, Bcl-2, and CL-Caspase-3 by Western blot. The results demonstrated that, compared to the SCI group, the rTSMS group showed lower expressions of Bax and CL-Caspase-3 proteins, especially in the 1 Hz group (BAX, P = 0.0038; CL-Caspase-3, P = 0.013), and higher Bcl-2 protein levels (P = 0.001), with the 1 Hz group outperforming the 20 Hz group (BAX, P = 0.0044; CL-Caspase-3, P = 0.0293; Bcl-2, P = 0.0289), as shown in Figure 2D–G.

Free radical release and oxidative stress levels increase after SCI, further damaging cells and tissues and exacerbating the injury.[29] We evaluated the activities of antioxidant enzymes SOD, CAT, and GSH-PX, along with the oxidative damage marker MDA. Compared to the SCI group, the rTSMS group exhibited higher SOD, CAT, and GSH-PX activities, particularly in the 1 Hz group (SOD, P = 0.0046; CAT, P = 0.0109; GSH-PX, P = 0.0021), and lower MDA levels (P = 0.0017), with 1 Hz being more effective than 20 Hz (SOD, P = 0.0282; CAT, P = 0.0468; GSH-PX, P = 0.0366; MDA, P = 0.00470), as shown in Figure 2H–K.

These findings indicate that rTSMS intervention can alleviate apoptosis, spinal edema, and oxidative stress after spinal cord injury, with 1 Hz being more effective than 20 Hz.

1 Hz rTSMS Inhibits NLRP3 Inflammasome Activation After SCI

To evaluate the effects of 1 Hz rTSMS on NLRP3 inflammasome activation after SCI, we performed Western blot and immunofluorescence staining to assess the temporal expression and cellular localization of key inflammasome-related proteins, including NLRP3, ASC, CL-Caspase-1, IL-1β, and IL-18, at 3, 7, 14, and 21 days post-injury.

Western blot analysis demonstrated a significant upregulation of NLRP3 inflammasome components in the SCI group across all time points, with peak expression observed at day 3. 1 Hz rTSMS substantially suppressed the expression of these proteins at each time point compared to the SCI group.Specifically, NLRP3 expression was significantly increased in the SCI group compared to Sham at day 3, and 1 Hz rTSMS significantly reduced NLRP3 levels at these time points (day 3, P = 0.0074; day 7, P = 0.034; day 14, P = 0.0056; day 21, P = 0.0142). Similarly, ASC protein levels were elevated in SCI at day 3, with significant suppression by 1 Hz rTSMS at each time point (day 3, P = 0.1743; day 7, P = 0.0102; day 14, P = 0.01; day 21, P = 0.0036). CL-Caspase-1 expression followed the same trend, showing significant increases in SCI vs Sham at day 3, and decreases after 1 Hz rTSMS treatment (day 3, P = 0.114; day 7, P = 0.0893; day 14, P = 0.0239; day 21, P = 0.0313). IL-1β levels were significantly upregulated in SCI at day 3, and markedly reduced following 1 Hz rTSMS intervention (day 3, P = 0.0068; day 7, P = 0.0002; day 14, P = 0.0001; day 21, P = 0.0001). Similarly, IL-18 expression was increased in SCI compared to Sham at day 3, and was significantly suppressed by 1 Hz

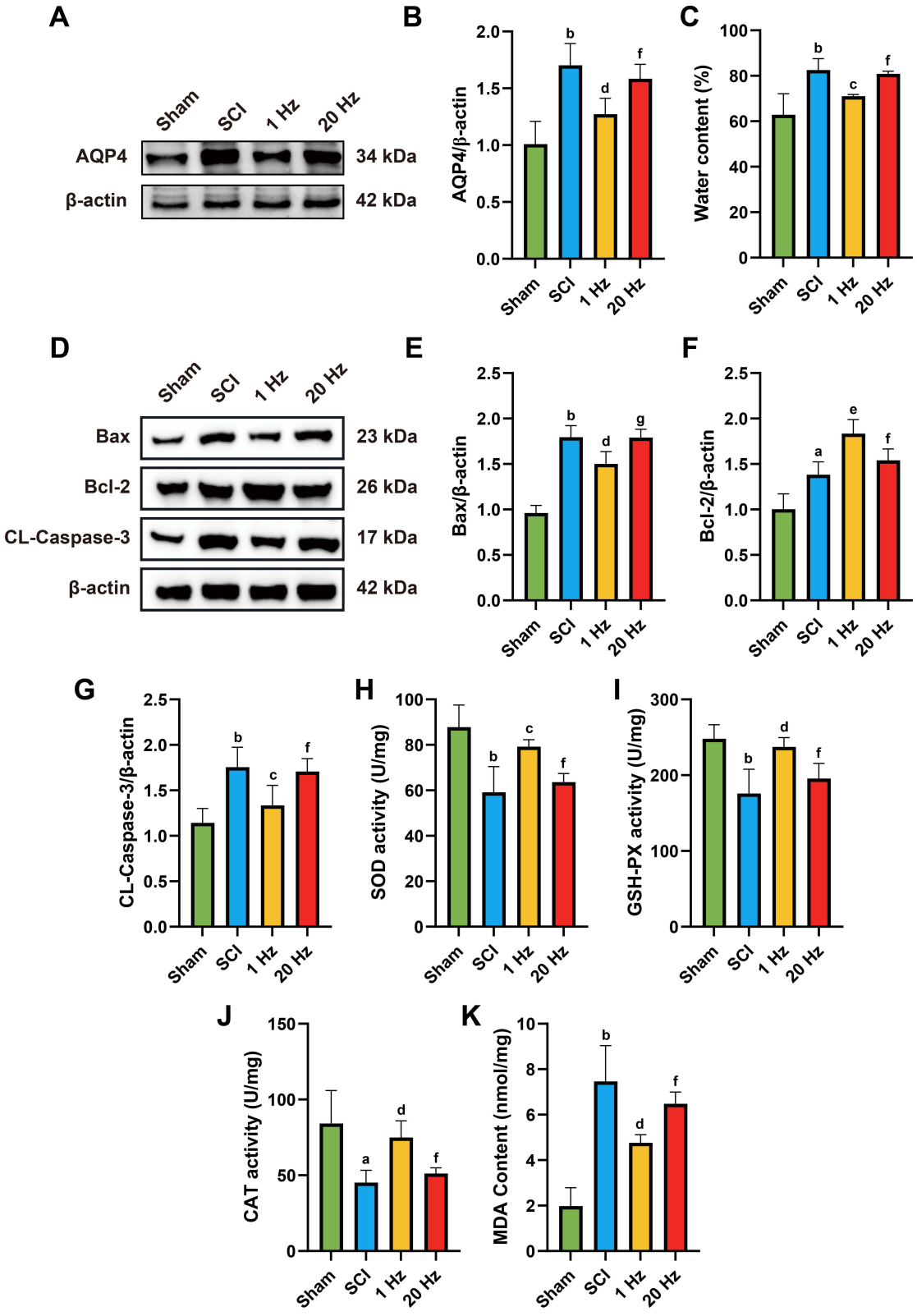

Figure 2 1 Hz rTSMS can alleviate complications such as spinal cord edema, oxidative stress, and apoptotic response after SCI. (**A** and **B**) Representative protein expression results and statistical analysis of AQP4 after SCI. (**C**) Statistical analysis of spinal cord water content. (**D-G**) Representative protein expression results (**D**) and statistical analysis of BAX (**E**), Bcl-2 (**F**), and CL-Caspase-3 (**G**) at the site of SCI.(**H-K**) Statistical analysis of SOD (**H**),GSH-PX (**I**), and CAT (**J**) activities at the site of SCI. (**K**) Statistical analysis of MDA content at the site of SCI. n=5. $^{a}P<0.01$, $^{b}P<0.001$, vs Sham group. $^{c}P<0.05$, $^{d}P<0.01$, $^{e}P<0.001$, vs SCI group. $^{f}P<0.05$, $^{g}P<0.01$, vs 1 Hz group. The data are expressed as the mean ± SD.

https://doi.org/10.2147/JIR.S516006

rTSMS at each time point (day 3, $P = 0.0034$; day 7, $P = 0.0081$; day 14, $P = 0.0001$; day 21, $P = 0.0002$), as shown in Figure 3A–F.

Consistent with these findings, immunofluorescence staining revealed abundant Iba-1$^+$and NLRP3$^+$ cells in the injured spinal cord at all examined stages, with a temporal pattern paralleling the protein expression data. Importantly, compared to the SCI group, 1 Hz rTSMS significantly reduced the number of Iba-1$^+$and NLRP3$^+$ cells at day 3 (1 Hz, $P = 0.0466$), day 7 (1 Hz, $P = 0.0287$), day 14 (1 Hz, $P = 0.0171$), and day 21 (1 Hz, $P = 0.0101$), as shown in Figure 4A–H, indicating effective attenuation of microglial NLRP3 inflammasome overactivation.

Although NLRP3 expression peaked between days 3 and 14 post-injury, behavioral assessments showed that motor function recovery was most prominent at day 21, exceeding earlier time points significantly. This suggests that despite the gradual decline of the inflammatory response, residual inflammasome activity may continue to impede neural repair. Thus, day 21 represents a critical stage in which inflammation tends to stabilize while functional recovery enters an important phase. This time point, characterized by a moderate inflammatory microenvironment, may provide a valuable window for neural plasticity and serve as an optimal time point for further mechanistic investigations.

1 Hz rTSMS Attenuates Astrocyte Activation and Pro-Inflammatory Responses While Promoting Neurotrophic and Anti-Inflammatory Signaling After SCI

To investigate the neuroinflammatory microenvironment following 1 Hz rTSMS intervention, we first assessed astrocyte activation via GFAP Immunofluorescence (IF) and Western blot analysis. SCI induced a marked increase in GFAP expression, indicative of reactive astrogliosis, whereas both 1 Hz rTSMS and MCC950 interventions significantly reduced GFAP levels (1 Hz, $P = 0.0036$, MCC950, $P = 0.0161$). Consistently, Western blot analysis confirmed down-regulation of GFAP protein expression in the 1 Hz and MCC950 groups (1Hz, $P = 0.0077$, MCC950, $P = 0.01$), as shown in Figure 5A–D

Next, we examined the expression of BDNF, a key molecule involved in neuronal survival and regeneration. Compared to the SCI group, both 1 Hz rTSMS and MCC950 significantly increased BDNF expression (1Hz, $P = 0.0029$, MCC950, $P = 0.0211$), as shown in Figure 5C and E, suggesting enhanced neurotrophic support in the injured spinal cord.

Furthermore, we analyzed the inflammatory microenvironment by assessing the expression of pro-inflammatory cytokines, including TNF-α, IFN-γ, and IL-6, as well as anti-inflammatory cytokines IL-4 and IL-10. SCI induced a robust upregulation of TNF-α, IFN-γ, and IL-6, as shown in Figure 5F–5I, whereas both 1 Hz rTSMS and MCC950 markedly suppressed their expression (TNF-α: 1Hz, $P = 0.0001$, MCC950, $P = 0.0156$; IFN-γ: 1Hz, $P = 0.0001$, MCC950, $P = 0.0036$; IL-6: 1Hz, $P = 0.0001$, MCC950, $P = 0.0409$). Conversely, the expression of IL-4 and IL-10 was significantly elevated in the 1 Hz and MCC950 groups compared to SCI (IL-4: 1Hz, $P = 0.0001$, MCC950, $P = 0.002$; IL-10: 1Hz, $P = 0.0103$, MCC950, $P = 0.0311$), as shown in Figure 5J and K, indicating a shift toward an anti-inflammatory profile.

These results suggest that 1 Hz rTSMS alleviates neuroinflammation and astrogliosis, while enhancing trophic and anti-inflammatory signaling, thereby creating a favorable microenvironment for neuronal survival and axonal regeneration following SCI.

1 Hz rTSMS Facilitates Neuronal Preservation and Axonal Regrowth After Spinal Cord Injury

To evaluate the effects of 1 Hz rTSMS on neuronal protection and axonal regeneration after SCI, we first performed NeuN immunofluorescence staining to assess neuronal survival in the ventral horn region of the spinal cord. The results showed that, compared with the Sham group, the number of NeuN$^+$ cells was significantly reduced in the SCI group, whereas both 1 Hz rTSMS and the NLRP3 inflammasome inhibitor MCC950 markedly increased the number of NeuN$^+$ cells (1 Hz, $P = 0.0016$; MCC950, $P = 0.0017$), as shown in Figure 6A and B, indicating that these interventions exert neuroprotective effects. To further assess the capacity for axonal regeneration, we employed retrograde tracing by injecting rAAV/Retro virus into the spinal cord to label cortical motor neurons. In the SCI group, the number of traced neurons was markedly reduced,

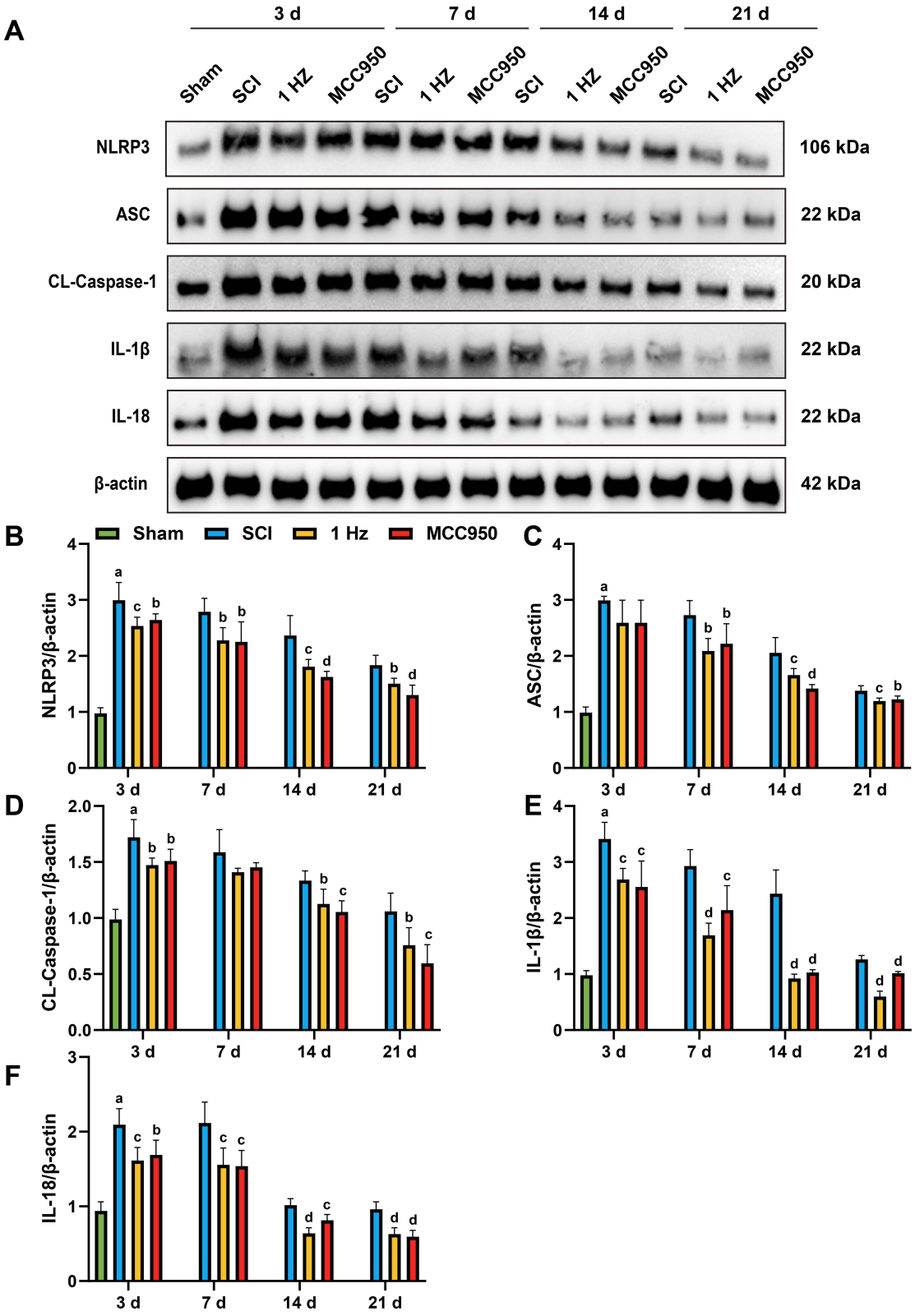

Figure 3 1 Hz rTSMS attenuates the expression of NLRP3 inflammasome-related proteins at 3, 7, 14 and 21 days post-injury. (**A**) Western blot analysis showing the expression of NLRP3, ASC, CL-Caspase-1, IL-1β, and IL-18 in the spinal cord tissue at 3, 7, 14, and 21 days post-injury. (**B**–**F**) Statistical graph of NLRP3 (**B**), ASC (**C**), CL-Caspase-1(**D**), IL-1β (**E**) and IL-18 (**F**) protein expression levels in each group at different time points. n=5. $^{a}P<0.001$, vs Sham group. $^{b}P<0.05$, $^{c}P<0.01$, $^{d}P<0.001$,vs SCI group. The data are expressed as the mean ± SD.

https://doi.org/10.2147/JIR.S516006

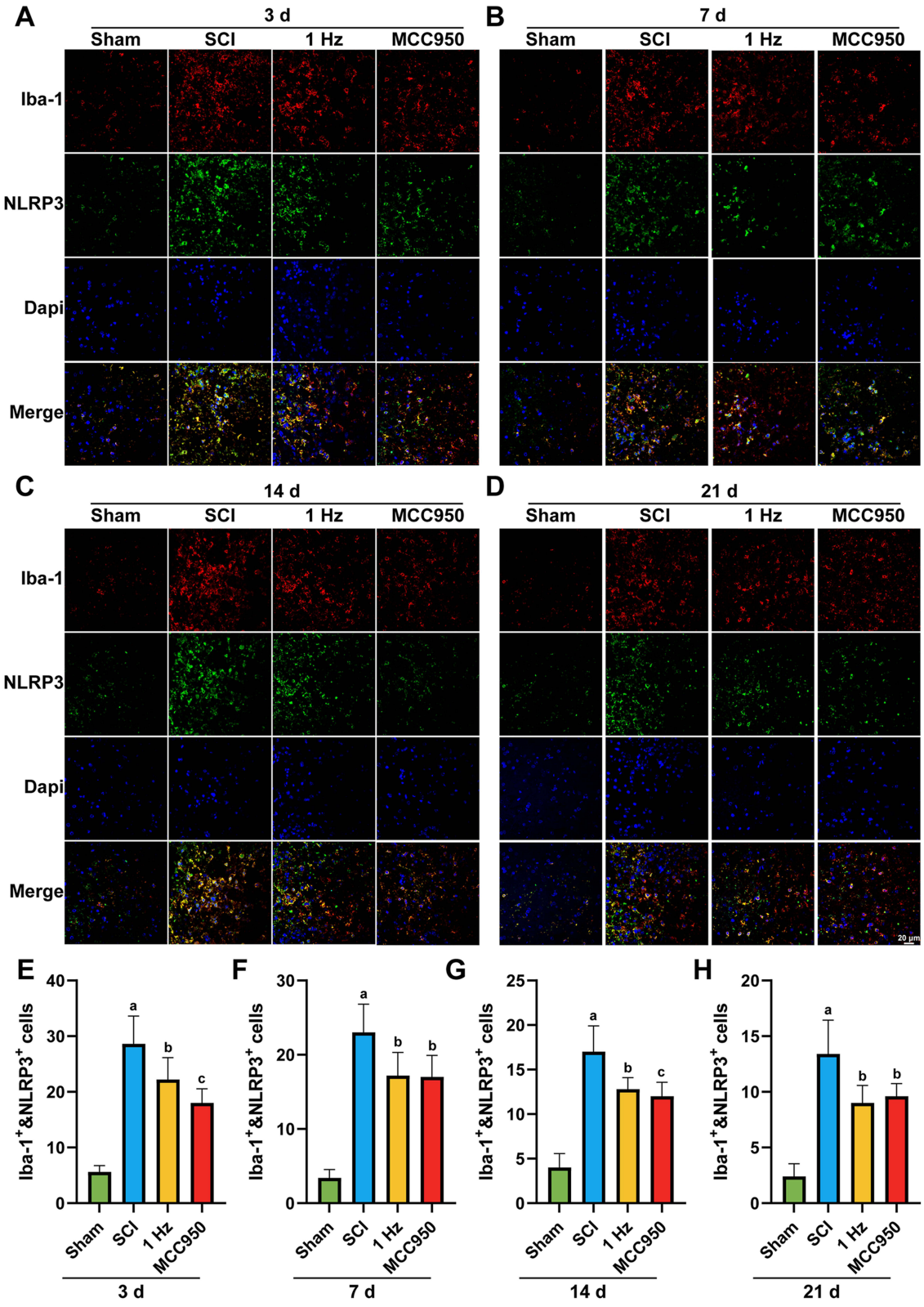

Figure 4 1 Hz rTSMS reduces NLRP3 inflammasome activation in microglia at different time points after spinal cord injury. (**A**–**D**) Representative immunofluorescence images showing co-localization of Iba-1 (red, a microglial marker) and NLRP3 (green) in the injured spinal cord at 3 (**A**), 7 (**B**), 14 (**C**), and 21 days (**D**) after injury in different groups. (**E**–**H**) Quantification of Iba-1$^+$&NLRP3$^+$ cells at 3 (**E**), 7 (**F**), 14 (**G**), and 21 days (**H**) after injury in different groups. n=5. Scale bar = 20 μm. ^{a}*P*<0.001, vs Sham group. ^{b}*P*<0.05, ^{c}*P*<0.01,vs SCI group. The data are expressed as the mean ± SD.

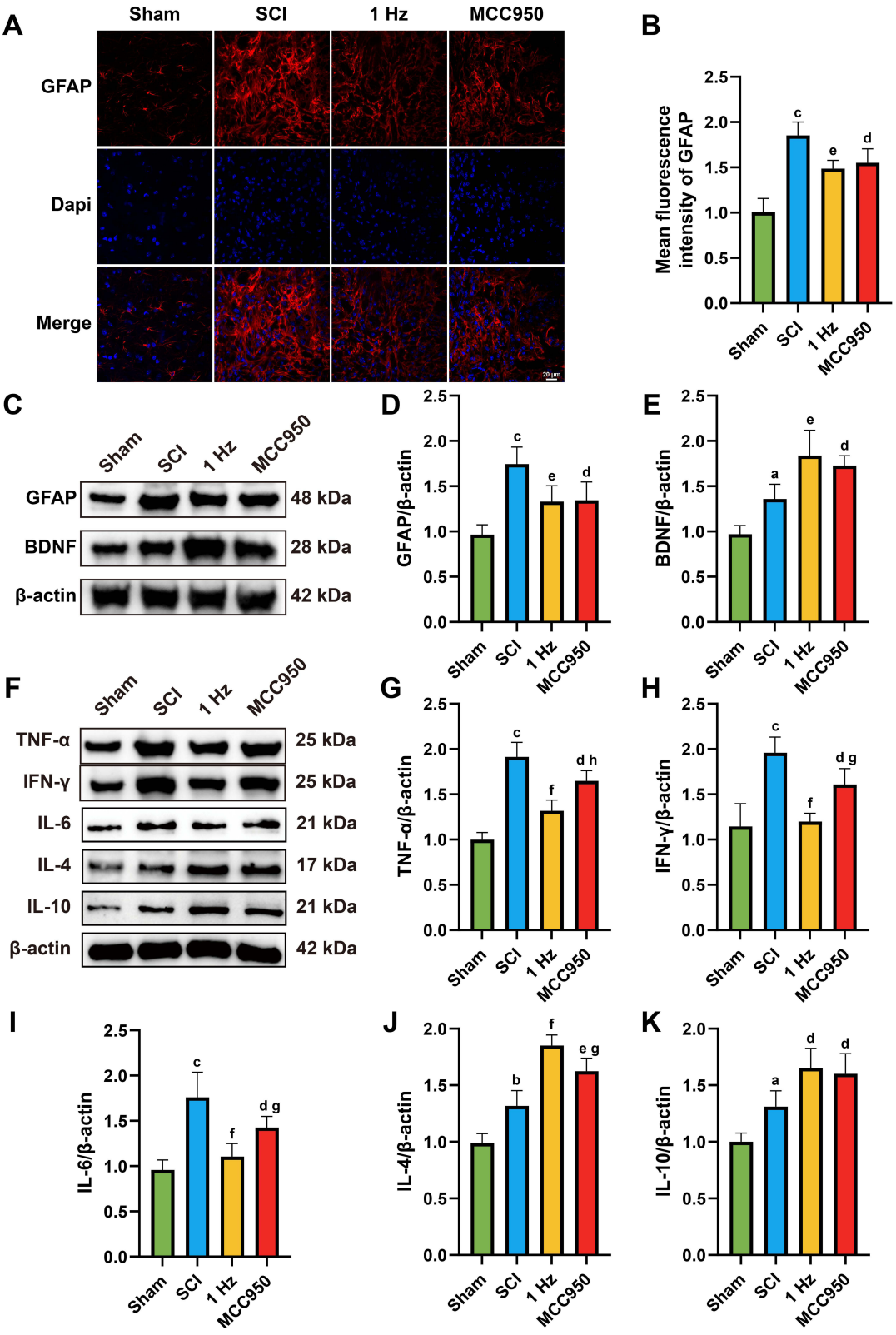

Figure 5 1 Hz rTSMS reduces astrocyte activation and neuroinflammation. (**A**) Representative immunofluorescence images showing GFAP (red) and Dapi (blue) staining in the injured spinal cord across groups. (**B**) Quantification of mean GFAP fluorescence intensity. (**C**) Western blot analysis of GFAP and BDNF expression. (**D** and **E**) Quantification of GFAP and BDNF relative to β-actin. (**F**) Western blot analysis of pro-inflammatory cytokines (TNF-α, IFN-γ and IL-6) and anti-inflammatory cytokines (IL-4 and IL-10). (**G**–**K**) Corresponding quantification of cytokine expression. n=5. Scale bar=20 μm. $^{a}P < 0.05$, $^{b}P < 0.01$, $^{c}P < 0.001$, vs Sham group. $^{d}P < 0.05$, $^{e}P < 0.01$, $^{f}P < 0.001$, vs SCI group. $^{g}P < 0.05$, $^{h}P < 0.01$, vs 1 Hz group. The data are expressed as the mean ± SD.

https://doi.org/10.2147/JIR.S516006

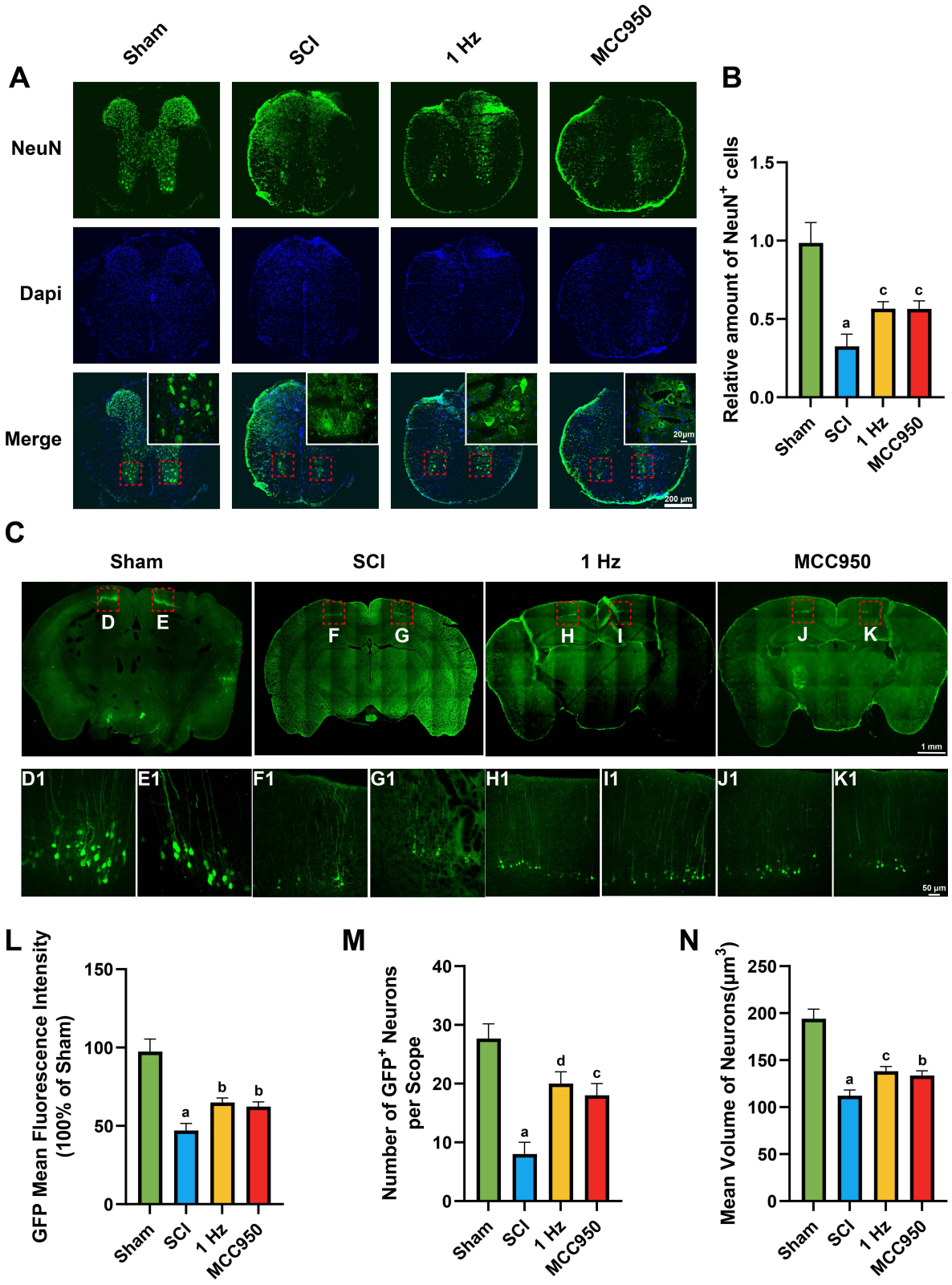

Figure 6 1 Hz rTSMS preserve neuronal survival and promote axonal regeneration after SCI. (**A**) Representative immunofluorescence images showing NeuN$^+$ neurons (green) and Dapi (blue) in transverse spinal cord sections at 21 days post-injury across four groups (Sham, SCI, 1 Hz rTSMS, MCC950). Scare bar=200 μm. Insets show higher magnification of ventral horn neurons. Scare bar=20 μm. (**B**) Quantification of NeuN$^+$ cells in the ventral horn area (n=6). (**C**) Representative images of cortical motor neurons retrogradely labeled by rAAV/Retro. Scare bar=1mm. (**D1**–**K1**) Display higher magnification images of the selected boxed regions. Scare bar=50 μm. (**L**) Quantification of GFP fluorescence intensity (n=3). (**M**) Number of GFP$^+$ neurons per field (n=3). (**N**) Mean volume of traced neurons (n=3). $^aP < 0.001$, vs Sham group. $^bP < 0.05$, $^cP < 0.01$, $^dP < 0.001$, vs SCI group. Data are presented as mean ± SD.

accompanied by irregular neuronal morphology, smaller somatic volume, and shortened or disrupted axons. Compared with the SCI group, both 1 Hz rTSMS and MCC950 significantly increased the GFP fluorescence intensity (1 Hz, $P = 0.011$; MCC950, $P = 0.0254$), number (1 Hz, $P = 0.0006$; MCC950, $P = 0.002$) and average volume (1 Hz, $P = 0.0075$; MCC950, $P = 0.0215$) of GFP^+ traced neurons, as shown in Figure 6C, (D1–K1) and L–N, suggesting that 1 Hz rTSMS has the potential to promote axonal regeneration and neuronal repair after SCI.

1 Hz MS Decreases the Expression of NLRP3 Inflammasome in BV2

Microglial cells possess essential components for activating the NLRP3 inflammasome. We utilized immunofluorescence and Western Blot to detect the expression of NLRP3 inflammasome-related components in BV2 cells, including NLRP3, ASC, cleaved caspase-1, IL-1β, and IL-18.

Immunofluorescence results showed that the expression levels of NLRP3 were significantly decreased in both the LPS+MS group ($P = 0.0046$) and LPS+MCC950 group ($P = 0.0255$) compared to the LPS group, as shown in Figure 7A and B.

Western blot analysis revealed consistent results. The protein expression of NLRP3 was significantly reduced in both the LPS+MS ($P = 0.0001$) and LPS+MCC950 ($P = 0.0312$) groups compared to the LPS group, with a further decrease observed in the LPS+MS group versus LPS+MCC950 ($P = 0.041$). Similarly, ASC expression was significantly decreased in the LPS+MS ($P = 0.0001$) and LPS+MCC950 ($P = 0.0444$) groups, with the LPS+MS group showing a further reduction compared to LPS+MCC950 ($P = 0.013$). ForCL-Caspase-1, protein levels were markedly lower in the LPS+MS ($P = 0.0001$) and LPS+MCC950 ($P = 0.0327$) groups versus LPS, with a further decline in LPS+MS compared to LPS+MCC950 ($P = 0.0489$). Expression of IL-1β was also significantly decreased in both the LPS+MS ($P = 0.0004$) and LPS+MCC950 ($P = 0.0045$) groups relative to LPS. Furthermore, IL-18 expression was significantly downregulated in the LPS+MS ($P = 0.0001$) and LPS+MCC950 ($P = 0.0388$) groups, with the LPS+MS group again showing a greater reduction compared to LPS+MCC950 ($P = 0.0412$), as shown in Figure 7C–H.

1 Hz MS Reduced the Expression of Proinflammatory Cytokines and Increased the Expression of Anti-Inflammatory Cytokines

In the LPS-induced BV2 cell injury model, ELISA was performed to detect pro-inflammatory cytokines. The expression of TNF-α was significantly reduced in the LPS+MS group ($P = 0.0049$) and LPS+MCC950 group ($P = 0.072$) compared to the LPS group, with a further reduction in the LPS+MS group compared to LPS+MCC950 ($P = 0.041$). Similarly, IL-6 levels were decreased in both the LPS+MS ($P = 0.0022$) and LPS+MCC950 ($P = 0.0237$) groups versus LPS. For IL-1β, the LPS+MS group ($P = 0.0001$) and LPS+MCC950 group ($P = 0.0178$) showed significantly lower expression compared to LPS, and the LPS+MS group also exhibited lower levels than the LPS+MCC950 group ($P = 0.0017$), as shown in Figure 8A–C.

Additionally, ELISA results indicated upregulation of anti-inflammatory cytokines. TGF-β1 levels were elevated in the LPS+MS ($P = 0.0012$) and LPS+MCC950 ($P = 0.0027$) groups versus the LPS group. IL-4 expression was also significantly increased in the LPS+MS ($P = 0.0001$) and LPS+MCC950 ($P = 0.0033$) groups relative to LPS, with the LPS+MS group showing higher levels than LPS+MCC950 ($P = 0.0368$). For IL-10, levels were markedly upregulated in both LPS+MS ($P = 0.0001$) and LPS+MCC950 ($P = 0.0017$) groups, and the increase was more pronounced in the LPS +MS group compared to LPS+MCC950 ($P = 0.0473$), as shown in Figure 8D–F.

1 Hz MS Improves PC12 Survival Through Inhibition of the NLRP3 Inflammasome

To determine whether the reduction of NLRP3 inflammasome in BV2 exerts neuroprotective effects on PC12 cells, we collected culture supernatants from various groups of BV2 cells (centrifuged at 5000g for 10 minutes, and supernatants collected) to culture PC12 cells. Subsequently, we used immunofluorescence to detect the expression of neuronal markers MAP2 and β-III-tubulin, CCK8 assay to assess PC12 cell viability, and measured LDH release.

Results showed that the expression levels of MAP2, β-III-tubulin and cell viability in the MS BV2-CM group and MCC950 BV2-CM group were higher than those in the LPS group (MAP2: MS BV2-CM group, P =0.0001, MCC950 BV2-CM group, P =0.0401; β-III-tubulin: MS BV2-CM group, P =0.0001, MCC950 BV2-CM group, P =0.046; cell

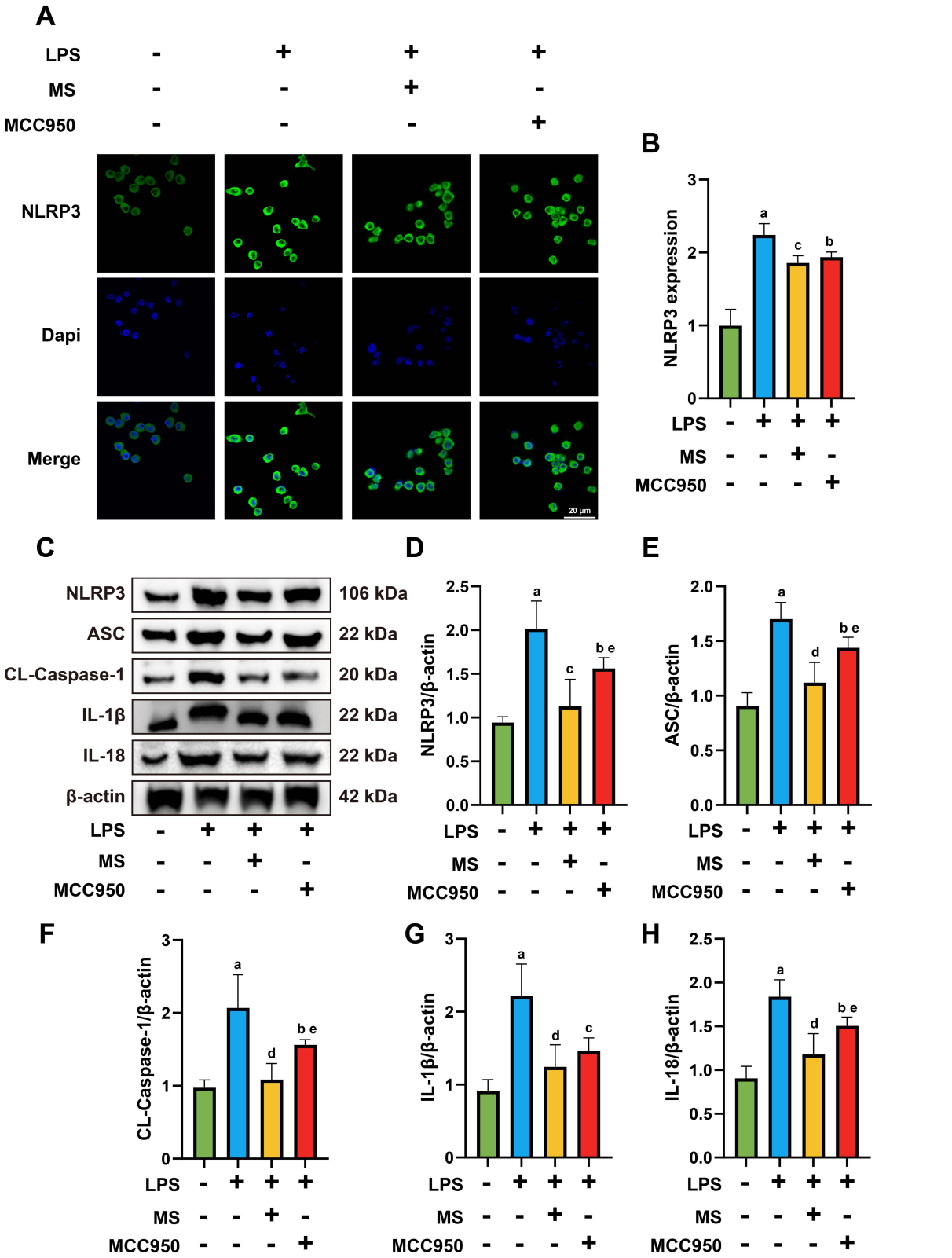

Figure 7 1 Hz MS attenuate the expression of NLRP3 in the LPS-induced BV2 injury model. (**A** and **B**) Immunofluorescence staining results and statistical analysis of NLRP3 in BV2 cells following MS intervention. (**C-H**) Representative images of protein expression of NLRP3 (**D**), ASC (**E**), CL-Caspase-1 (**F**), IL-1β (**G**), and IL-18 (**H**) and quantitative analysis. n=5. Scale bar=20 μm. [a]*P*<0.05, vs Con group. [b]*P*<0.05, [c]*P*<0.01, [d]*P*<0.001, vs LPS group. [e]*P*<0.05, vs LPS+MS group. The data are expressed as the mean ± SD.

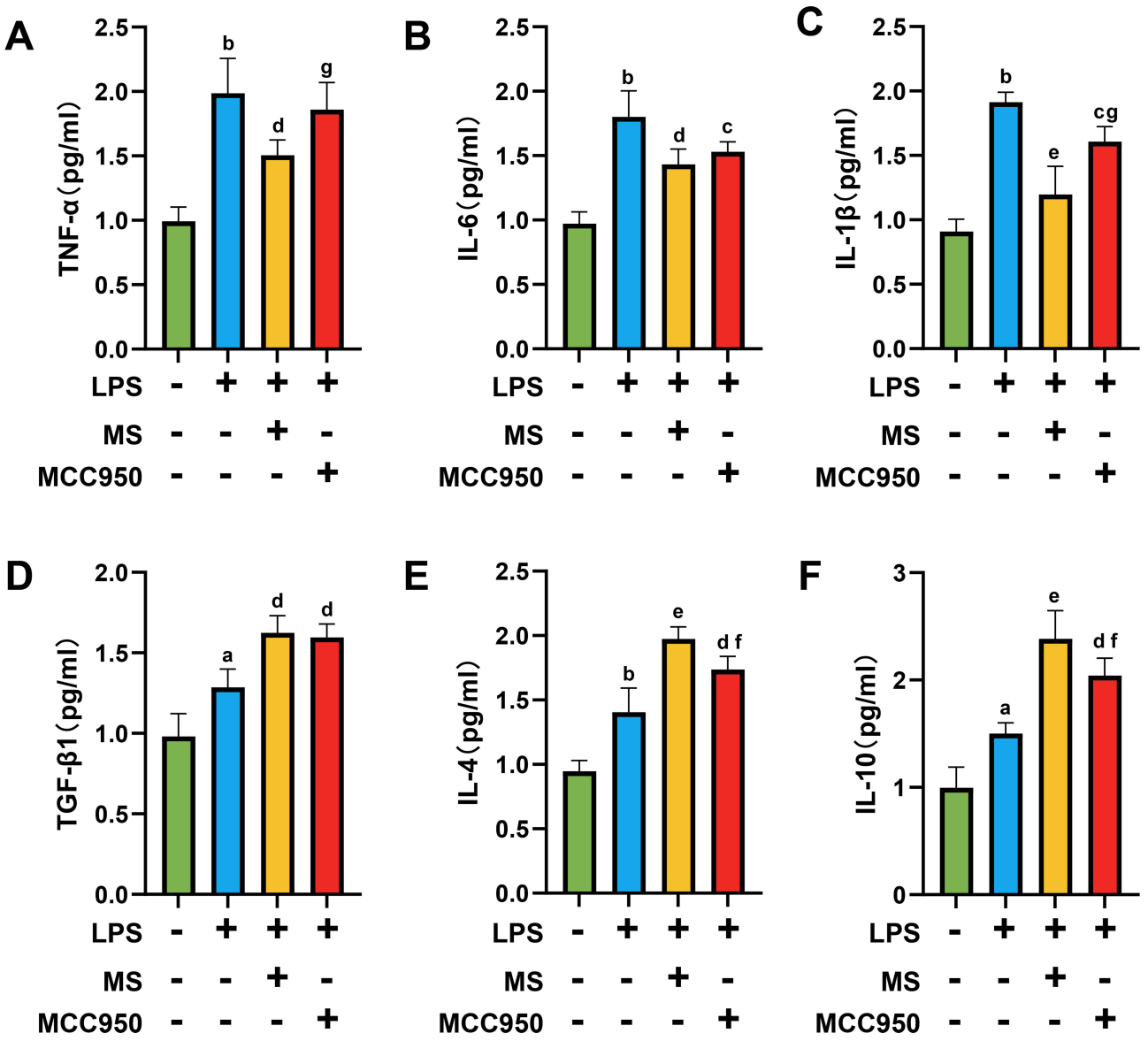

Figure 8 1Hz MS reduced the release of pro-inflammatory cytokines and enhanced the release of anti-inflammatory cytokines in the BV2 injury model. (**A-C**) Statistical graphs of ELISA assays showing the release of pro-inflammatory cytokines TNF-α (**A**), IL-6 (**B**), and IL-1β (**C**) from BV2 cells. (**D–F**) Statistical graphs of ELISA assays showing the release of pro-inflammatory cytokines TGF-β1 (**D**), IL-4 (**E**), and IL-10 (**F**) from BV2 cells. n=5. $^{a}P<0.01$, $^{b}P<0.001$, vs Con group. $^{c}P<0.05$, $^{d}P<0.01$, $^{e}P<0.001$, vs LPS group. $^{f}P<0.05$, $^{g}P<0.01$, vs LPS+MS group. The data are expressed as the mean ± SD.

viability: MS BV2-CM group, P =0.0001, MCC950 BV2-CM group, P =0.0451). Furthermore, the MS BV2-CM group exhibited significantly higher expression of MAP2 (P = 0.0473), β-III-tubulin (P = 0.0479) and cell viability (P = 0.0313) compared to the MCC950 BV2-CM group, as shown in Figure 9A–E.

Additionally, compared to the LPS group, the levels of LDH release was decreased in both MS BV2-CM group (P = 0.0001) and MCC950 BV2-CM group (P = 0.0041), with the MS BV2-CM group showing a greater decrease (P = 0.0003), as shown in Figure 9F.

Discussion

This study aimed to investigate the effects of rTSMS on motor function in mice after SCI and explore its underlying mechanisms. Our findings reveal that rTSMS can reduce neuroinflammation induces by SCI through activation of the

https://doi.org/10.2147/JIR.S516006

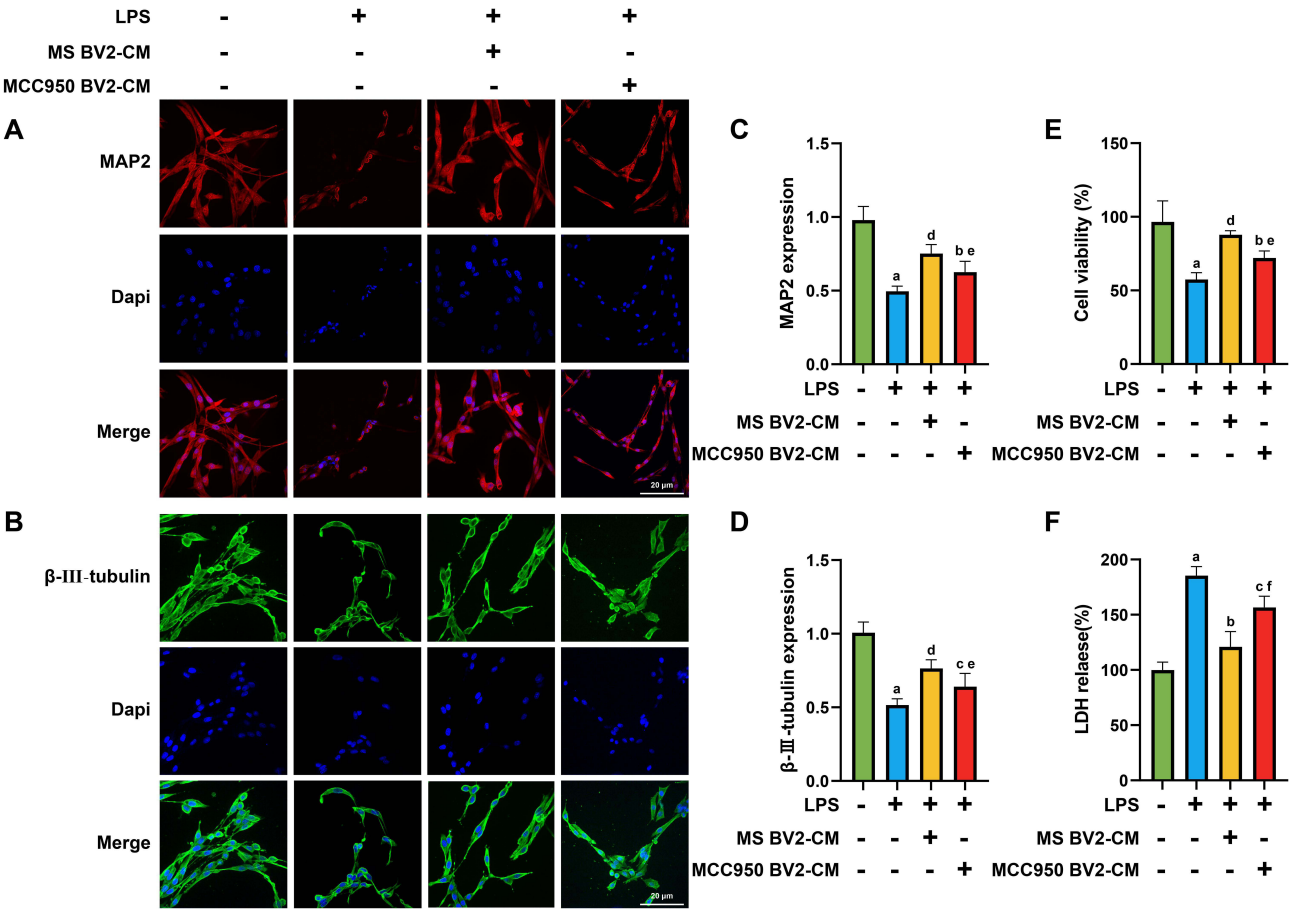

Figure 9 1 Hz MS exhibits a protective effect on injured PC12 cells. (**A**–**D**) Immunofluorescence images and statistical graphs of IF assays for the PC12 cell markers MAP2 and β-III-tubulin. (**E** and **F**) Statistical graphs of PC12 cell viability rates and LDH release levels in each group. n=5. Scale bar=20 μm. [a]*P*<0.001, vs Con group. [b]*P*<0.05, [c]*P*<0.01, [d]*P*<0.001, vs LPS group. [e]*P*<0.05, [f]*P*<0.01, vs LPS+MS BV2-CM group. The data are expressed as the mean ± SD.

NLRP3 inflammasome. Pharmacological inhibition of NLRP3 using the specific inhibitor MCC950 further demonstrated reductions in neuroinflammation, leading to neuroprotective effects and improved motor function in SCI mice. And similar results were obtained in in vitro experiments. Our research offers new insights into how rTSMS prevents neuronal damage post-SCI, suggesting that targeting NLRP3 could represent a novel therapeutic approach for SCI treatment.

In the rehabilitation therapy of SCI, inhibiting inflammatory responses and promoting neuronal protection are considered crucial for reversing motor dysfunction. To mitigate the side effects associated with SCI surgery and drug treatments,[30] a deeper understanding of the neuroinflammatory responses in SCI and the development of novel therapies to safeguard neurons from damage are essential.

Compared to traditional drug therapies, repetitive Transcranial Magnetic Stimulation (rTMS) offers unique advantages as a non-invasive method.[31] We applied rTMS directly to the site of spinal cord injury, termed rTSMS, to investigate its direct impact on spinal cord injury. Recent studies have highlighted rTMS's potential to exert anti-neuroinflammatory effects and promote neuronal protection,[32] which is particularly significant for central nervous system diseases such as SCI, stroke, Alzheimer's disease, and Parkinson's disease. For example, a meta-analysis has demonstrated that post-stroke rTMS application enhances motor function.[33] In Alzheimer's disease, rTMS is considered a promising neuroregulatory therapy that enhances cognitive function.[34] Literature reports suggest that rTMS contributes to improvements in motor function, with 1 Hz rTMS specifically identified as a beneficial strategy for motor recovery in subacute stroke patients,[35] Similarly, our data indicate that applying low-frequency 1 Hz rTSMS in the SCI region enhances hind limb motor function in SCI mice. Here, we speculate on why the effectiveness of low-frequency 1 Hz treatment is superior to 20 Hz in SCI mice., **i**: Low-frequency magnetic stimulation is typically associated with inhibitory

postsynaptic potentials, whereas high-frequency stimulation is associated with excitatory postsynaptic potentials. In the spinal cord injury mouse model, excessive excitatory postsynaptic potentials may be present, contributing to abnormal neural signal transmission and neuronal damage. Low-frequency 1 Hz stimulation may help mitigate this abnormal excitability, thereby potentially reducing further damage or facilitating repair processes. **ii**: Some studies suggest that low-frequency magnetic stimulation has neuroprotective effects, potentially alleviating neuronal death and inflammatory responses caused by spinal cord injury. This protective effect may be attributed to the inhibitory effects of low-frequency magnetic stimulation on neurons and its enhancement of neurotrophic factors, which help maintain neuronal health. **iii**: Spinal cord injury disrupts the normal function of neuronal circuits, leading to abnormal signal transmission and motor impairments. Low-frequency magnetic stimulation may improve motor recovery and neuronal regeneration by modulating the function of damaged neuronal circuits. In contrast, high-frequency magnetic stimulation may increase the excitability of neuronal circuits, exacerbating abnormal signal transmission and injury.

Microglia, as resident macrophages in the central nervous system, play a crucial role in neuroinflammation.[36] Our research has revealed a significant increase in microglial cell numbers following spinal cord injury, which can be mitigated with rTSMS intervention. Studies have indicated that microglia serve as a pivotal platform for the activation of the NLRP3 inflammasome, as they exclusively express all the proteins necessary for its formation.[36] Additionally, microglia are the primary source of inflammatory cytokines (such as TNF-α, IFN-γ, IL-1β, IL-6, and IL-18) associated with NLRP3 inflammasome. We measured the expression levels of these cytokines and observed increases in their levels in SCI group, which were reduced following treatment with the NLRP3 inflammasome inhibitor MCC950. Therefore, we hypothesize that in spinal cord injury, microglia play a central role in promoting the activation of NLRP3 inflammasomes, which in turn acts as a major driver of the inflammatory response.

Research has found that activation of the NLRP3 inflammasome exacerbates inflammatory responses, resulting in neuronal damage and neuroinflammation. This process may potentially impair neuronal function and contribute to neurodegenerative changes in the nervous system. For instance, in ischemia-reperfusion injury following cerebral artery occlusion, levels of inflammasome-related proteins significantly increase. This disruption can lead to compromised blood-brain barrier integrity, exacerbating inflammatory responses and neuronal injury.[37,38] After spinal cord injury, there is an increase in microglial cells and inflammasome activity in the injured area, which underscores the significance of NLRP3 inflammasomes in inflammatory responses. Studies indicate that utilizing NLRP3 inflammasome inhibitors, such as MCC950, can offer neuroprotection after SCI, thus potentially improving motor dysfunction.[39] Our research further supports this finding, demonstrating that rTSMS application after SCI reduces the expression of NLRP3 inflammasome-related proteins, mirroring the neuroprotective effect observed with MCC950. Additionally, immunofluorescence staining of the neuronal marker NeuN at the SCI site indicates that rTSMS exerts a neuroprotective effect comparable to MCC950.

Although the role of non-invasive magnetic stimulation techniques in improving motor function after spinal cord injury has been reported, the underlying mechanisms remain not fully elucidated. Our study reveals that rTSMS modulates the activation platform of NLRP3 inflammasomes in microglial cells, thereby inhibiting inflammatory responses and exerting neuroprotective effects. This highlights a significant mechanism in the field of basic medical research. Although some experiments have shown promising results, several restrictive issues still need to be addressed in future work. Firstly, after SCI, astrocytes and oligodendrocytes are recruited to the injury site and play respective roles. However, their relationship with NLRP3 inflammasomes was not elucidated in this study. Secondly, peripheral monocytes/macrophages are also recruited to the spinal cord injury area post-SCI and play roles similar to microglial cells, but there are currently no effective means to distinguish between microglial cells and macrophages. Lastly, there are differences in the distribution patterns of microglial cells between rodent brains and human brains, which could increase the difficulty of translating basic research findings to clinical applications in the future.

Despite the promising neuroprotective effects of 1 Hz rTSMS in the SCI mouse model, clinical translation remains challenging. A major obstacle lies in the anatomical and physiological differences between the rodent and human spinal cord, including spinal size, depth, and tissue composition, which complicate direct extrapolation of stimulation parameters. Moreover, optimal rTSMS parameters for humans—such as dosage, frequency, and duration—are still unclear and warrant systematic clinical investigation.

Additionally, it is essential to conduct comparative analyses between 1 Hz rTSMS and FDA-approved neuromodulation devices, such as spinal cord stimulators (SCS)[40] and conventional transcranial magnetic stimulation (TMS),[41] to better define the clinical niche of rTSMS in SCI management. Unlike SCS, which requires surgical implantation and mainly modulates dorsal column pathways,[42] rTSMS is a noninvasive intervention that targets the lesion site through externally applied magnetic fields and may exert more direct effects on inflammation and axonal repair.[22] Compared to conventional TMS, which is primarily used for cortical modulation, rTSMS offers improved targeting precision and deeper tissue penetration, making it more suitable for local spinal cord modulation.[43,44] A systematic comparison of these modalities in terms of efficacy, safety, procedural simplicity, and cost-effectiveness will be crucial to evaluate the translational value of rTSMS.

Furthermore, exploring the synergistic potential between rTSMS and conventional rehabilitation strategies—including physical therapy, locomotor training, and neuromuscular electrical stimulation—is of paramount importance. Rehabilitation has been shown to promote activity-dependent neuroplasticity and circuit remodeling,[45] whereas rTSMS may optimize the microenvironment by suppressing inflammation and enhancing regeneration.[21,46] Integrating rTSMS into the rehabilitation process (eg, preceding or synchronizing magnetic stimulation with training) could enhance responsiveness to therapy and amplify overall functional recovery. Emerging evidence supports the superiority of multimodal interventions in CNS repair, making combination therapies a promising direction for future studies.

Future research should focus on optimizing rTSMS stimulation protocols tailored to human anatomy and physiology, including magnetic field intensity, coil positioning, frequency, and duration. Long-term safety assessments are also needed to evaluate potential off-target effects, plasticity-related consequences, and adverse outcomes. Advancing the clinical translation of rTSMS will require interdisciplinary collaboration among neuroscientists, rehabilitation specialists, biomedical engineers, and clinicians to develop standardized and individualized treatment regimens. Ultimately, the integration of rTSMS into multidisciplinary rehabilitation programs may offer a novel and effective therapeutic strategy for patients with SCI.

In summary, our study demonstrates that 1 Hz rTSMS can inhibit microglia, reduce NLRP3 inflammasome activation, alleviate inflammatory responses, and promote motor function recovery in mice after spinal cord injury. These findings offer new perspectives and strategies for treating spinal cord injury and provide a theoretical foundation for the future clinical application of rTSMS.

Conclusions

1 Hz rTSMS reduces NLRP3 inflammasome activation, improve spinal cord injury outcomes, suppress inflammatory responses, exert neuroprotective effects, and promote motor function recovery in SCI mice.

Highlights

1. 1 Hz rTSMS significantly improves hindlimb motor function recovery after spinal cord injury.
2. 1 Hz rTSMS inhibits NLRP3 inflammasome activation, reducing neuroinflammatory responses.
3. 1 Hz rTSMS increases NeuN, MAP2 and β-III-tubulin expression, promoting neuroprotection.

Acknowledgments

We thank Dr. Ying-nan Song, Translational Medicine Research Center of Guizhou Medical University and Dr. Da-quan Sun, Research Center for Basic Sciences of Medicine of Guizhou Medical University for their technical assistance.

Authors' Contributions

All authors made a significant contribution to the work reported, whether that is in the conception, study design, execution, acquisition of data, analysis and interpretation, or in all these areas; took part in drafting, revising or critically reviewing the article; gave final approval of the version to be published; have agreed on the journal to which the article has been submitted; and agree to be accountable for all aspects of the work.

Funding

The study was supported by the Science and Technology Planning Foundation of Guizhou Province (QKH - ZK - [2021]-General 472, ZK - [2024]-General 120); Guizhou Health Commission Scientific and Technological Fund Program (gzwkj2025-077); The PhD research start-up Foundation of Guizhou Medical University (XBH - J - [2020]-009); The Youth Science and Technology personnel training Foundation of Guizhou Provincial Education Department (QJH - KY - [2022]-226).

Disclosure

The authors have declared that no competing interest exists in this work.

References

1. Ahuja CS, Nori S, Tetreault L, et al. Traumatic spinal cord injury-repair and regeneration. *Neurosurgery*. 2017;80(3s):S9–s22. doi:10.1093/neuros/nyw080
2. Qin W, Luo H, Yang L, et al. Rubia cordifolia L. ameliorates DSS-induced ulcerative colitis in mice through dual inhibition of NLRP3 inflammasome and IL-6/JAK2/STAT3 pathways. *Heliyon*. 2022;8(8):e10314. doi:10.1016/j.heliyon.2022.e10314
3. Shirinpour S, Hananeia N, Rosado J, et al. Multi-scale modeling toolbox for single neuron and subcellular activity under transcranial magnetic stimulation. *Brain Stimul*. 2021;14(6):1470–1482. doi:10.1016/j.brs.2021.09.004
4. Bai YW, Yang QH, Chen PJ, Wang XQ. Repetitive transcranial magnetic stimulation regulates neuroinflammation in neuropathic pain. *Front Immunol*. 2023;14:1172293. doi:10.3389/fimmu.2023.1172293
5. Medina-Fernández FJ, Escribano BM, Padilla-Del-Campo C, Drucker-Colín R, Pascual-Leone Á, Túnez I. Transcranial magnetic stimulation as an antioxidant. *Free Radic Res*. 2018;52(4):381–389. doi:10.1080/10715762.2018.1434313
6. Dufor T, Grehl S, Tang AD, et al. Neural circuit repair by low-intensity magnetic stimulation requires cellular magnetoreceptors and specific stimulation patterns. *Sci Adv*. 2019;5(10):eaav9847. doi:10.1126/sciadv.aav9847
7. Zewdie E, Ciechanski P, Kuo HC, et al. Safety and tolerability of transcranial magnetic and direct current stimulation in children: prospective single center evidence from 3.5 million stimulations. *Brain Stimul*. 2020;13(3):565–575. doi:10.1016/j.brs.2019.12.025
8. Luk KY, Ouyang HX, Pang MYC. Low-Frequency rTMS over contralesional m1 increases ipsilesional cortical excitability and motor function with decreased interhemispheric asymmetry in subacute stroke: a randomized controlled study. *Neural Plast*. 2022;2022:3815357. doi:10.1155/2022/3815357
9. Jiang G, Song H, Han X, et al. Low frequency of repetitive trans-spinal magnetic stimulation promotes functional recovery after spinal cord injury in mice through inhibiting TGF-β1/Smad2/3 signaling pathway. *Neurosci Lett*. 2024;836:137890. doi:10.1016/j.neulet.2024.137890
10. Ishikawa H, Shindo A, Ii Y, et al. MEFV gene mutations in neuro-Behçet's disease and neuro-Sweet disease. *Ann Clin Transl Neurol*. 2019;6(12):2595–2600. doi:10.1002/acn3.50937
11. Müller N, Scheld M, Voelz C, et al. Lipocalin-2 Deficiency Diminishes Canonical NLRP3 Inflammasome Formation and IL-1β Production in the Subacute Phase of Spinal Cord Injury. *Int J Mol Sci*. 2023;24(10):8689–8706. doi:10.3390/ijms24108689
12. Zhao W, Ma L, Cai C, Gong X. Caffeine Inhibits NLRP3 inflammasome activation by suppressing MAPK/NF-κB and A2aR Signaling in LPS-Induced THP-1 macrophages. *Int J Biol Sci*. 2019;15(8):1571–1581. doi:10.7150/ijbs.34211
13. Li Y, Li J, Yu Q, Ji L, Peng B. METTL14 regulates microglia/macrophage polarization and NLRP3 inflammasome activation after ischemic stroke by the KAT3B-STING axis. *Neurobiol Dis*. 2023;185:106253. doi:10.1016/j.nbd.2023.106253
14. Moonen S, Koper MJ, Van Schoor E, et al. Pyroptosis in Alzheimer's disease: cell type-specific activation in microglia, astrocytes and neurons. *Acta Neuropathol*. 2023;145(2):175–195. doi:10.1007/s00401-022-02528-y
15. Qiu J, Chen Y, Zhuo J, et al. Urolithin A promotes mitophagy and suppresses NLRP3 inflammasome activation in lipopolysaccharide-induced BV2 microglial cells and MPTP-induced Parkinson's disease model. *Neuropharmacology*. 2022;207:108963. doi:10.1016/j.neuropharm.2022.108963
16. Naeem A, Prakash R, Kumari N, et al. MCC950 reduces autophagy and improves cognitive function by inhibiting NLRP3-dependent neuroinflammation in a rat model of Alzheimer's disease. *Brain Behav Immun*. 2024;116:70–84. doi:10.1016/j.bbi.2023.11.031
17. Chen KP, Hua KF, Tsai FT, et al. A selective inhibitor of the NLRP3 inflammasome as a potential therapeutic approach for neuroprotection in a transgenic mouse model of Huntington's disease. *J Neuroinflammation*. 2022;19(1):56–72. doi:10.1186/s12974-022-02419-9
18. Wu X, Wang B, Zhou Y, et al. NLRP3 inflammasome inhibitor MCC950 reduces cerebral ischemia/reperfusion induced neuronal ferroptosis. *Neurosci Lett*. 2023;795:137032. doi:10.1016/j.neulet.2022.137032
19. Ismail EN, Jantan I, Vidyadaran S, Jamal JA, Azmi N. Phyllanthus amarus prevents LPS-mediated BV2 microglial activation via MyD88 and NF-κB signaling pathways. *BMC Complement Med Ther*. 2020;20(1):202–214. doi:10.1186/s12906-020-02961-0
20. Hou B, Yin J, Liu S, et al. Inhibiting the NLRP3 Inflammasome with MCC950 alleviates neurological impairment in the brain of EAE Mice. *Mol Neurobiol*. 2024;61(3):1318–1330. doi:10.1007/s12035-023-03618-y
21. Chalfouh C, Guillou C, Hardouin J, et al. The regenerative effect of trans-spinal magnetic stimulation after spinal cord injury: mechanisms and pathways underlying the effect. *Neurotherapeutics*. 2020;17(4):2069–2088. doi:10.1007/s13311-020-00915-5
22. Robac A, Neveu P, Hugede A, et al. Repetitive Trans Spinal Magnetic Stimulation Improves Functional Recovery and Tissue Repair in Contusive and Penetrating Spinal Cord Injury Models in rats. *Biomedicines*. 2021;9(12):1827–1843. doi:10.3390/biomedicines9121827
23. Kim SK, Lee GY, Kim SK, et al. protective effects of repetitive transcranial magnetic stimulation against streptozotocin-induced alzheimer's disease. *Mol Neurobiol*. 2024;61(3):1687–1703. doi:10.1007/s12035-023-03573-8
24. Jiao J, Zhao G, Wang Y, Ren P, Wu M. MCC950, a Selective Inhibitor of NLRP3 inflammasome, reduces the inflammatory response and improves neurological outcomes in mice model of spinal cord injury. *Front Mol Biosci*. 2020;7:37–46. doi:10.3389/fmolb.2020.00037

25. Lemarchand E, Barrington J, Chenery A, et al. Extent of Ischemic brain injury after thrombotic stroke is Independent of the NLRP3 (NACHT, LRR and PYD domains-containing protein 3) inflammasome. *Stroke*. 2019;50(5):1232–1239. doi:10.1161/strokeaha.118.023620
26. Chen B, Tan Q, Zhao W, et al. Diffusion tensor imaging and electrophysiology as robust assays to evaluate the severity of acute spinal cord injury in rats. *BMC Neurol*. 2020;20(1):236–245. doi:10.1186/s12883-020-01778-1
27. Kitchen P, Salman MM, Halsey AM, et al. targeting aquaporin-4 subcellular localization to treat central nervous system edema. *Cell*. 2020;181 (4):784–799. doi:10.1016/j.cell.2020.03.037
28. Xiao S, Zhang Y, Liu Z, et al. Alpinetin inhibits neuroinflammation and neuronal apoptosis via targeting the JAK2/STAT3 signaling pathway in spinal cord injury. *CNS Neurosci Ther*. 2023;29(4):1094–1108. doi:10.1111/cns.14085
29. Ge MH, Tian H, Mao L, et al. Zinc attenuates ferroptosis and promotes functional recovery in contusion spinal cord injury by activating Nrf2/GPX4 defense pathway. *CNS Neurosci Ther*. 2021;27(9):1023–1040. doi:10.1111/cns.13657
30. Bagnato GL, Miceli G, Marino N, Sciortino D, Bagnato GF. Pulsed electromagnetic fields in knee osteoarthritis: a double blind, placebo-controlled, randomized clinical trial. *Rheumatology*. 2016;55(4):755–762. doi:10.1093/rheumatology/kev426
31. Guidetti M, Bertini A, Pirone F, et al. Neuroprotection and Non-Invasive Brain Stimulation: facts or Fiction? *Int J Mol Sci*. 2022;23(22):13775–13791. doi:10.3390/ijms232213775
32. Clarke D, Beros J, Bates KA, Harvey AR, Tang AD, Rodger J. Low intensity repetitive magnetic stimulation reduces expression of genes related to inflammation and calcium signalling in cultured mouse cortical astrocytes. *Brain Stimul*. 2021;14(1):183–191. doi:10.1016/j.brs.2020.12.007
33. Hofmeijer J, Ham F, Kwakkel G. Evidence of rTMS for motor or cognitive stroke recovery: hype or hope? *Stroke*. 2023;54(10):2500–2511. doi:10.1161/strokeaha.123.043159
34. Velioglu HA, Dudukcu EZ, Hanoglu L, Guntekin B, Akturk T, Yulug B. rTMS reduces delta and increases theta oscillations in Alzheimer's disease: a visual-evoked and event-related potentials study. *CNS Neurosci Ther*. 2024;30(1):e14564. doi:10.1111/cns.14564
35. Gong Y, Long XM, Xu Y, Cai XY, Ye M. Effects of repetitive transcranial magnetic stimulation combined with transcranial direct current stimulation on motor function and cortex excitability in subacute stroke patients: a randomized controlled trial. *Clin Rehabil*. 2021;35(5):718–727. doi:10.1177/0269215520972940
36. Sochocka M, Ochnik M, Sobczyński M, et al. Ginkgo biloba leaf extract improves an innate immune response of peripheral blood leukocytes of alzheimer's disease patients. *Nutrients*. 2022;14(10):2022–2041. doi:10.3390/nu14102022
37. Li J, Xu P, Hong Y, et al. Lipocalin-2-mediated astrocyte pyroptosis promotes neuroinflammatory injury via NLRP3 inflammasome activation in cerebral ischemia/reperfusion injury. *J Neuroinflammation*. 2023;20(1):148–165. doi:10.1186/s12974-023-02819-5
38. Franke M, Bieber M, Kraft P, Weber ANR, Stoll G, Schuhmann MK. The NLRP3 inflammasome drives inflammation in ischemia/reperfusion injury after transient middle cerebral artery occlusion in mice. *Brain Behav Immun*. 2021;92:223–233. doi:10.1016/j.bbi.2020.12.009
39. He X, Yang W, Zeng Z, et al. NLRP3-dependent pyroptosis is required for HIV-1 gp120-induced neuropathology. *Cell Mol Immunol*. 2020;17 (3):283–299. doi:10.1038/s41423-019-0260-y
40. Ho JS, Poon C, North R, Grubb W, Lempka S, Bikson M. A visual and narrative timeline review of spinal cord stimulation technology and US food and drug administration milestones. *Neuromodulation*. 2024;27(6):1020–1025. doi:10.1016/j.neurom.2024.05.006
41. Han S, Li XX, Wei S, et al. Orbitofrontal cortex-hippocampus potentiation mediates relief for depression: a randomized double-blind trial and TMS-EEG study. *Cell Rep Med*. 2023;4(6):101060. doi:10.1016/j.xcrm.2023.101060
42. Yeung AM, Huang J, Nguyen KT, et al. Spinal cord stimulation for painful diabetic neuropathy. *J Diabetes Sci Technol*. 2024;18(1):168–192. doi:10.1177/19322968221133795
43. Klomjai W, Katz R, Lackmy-Vallée A. Basic principles of transcranial magnetic stimulation (TMS) and repetitive TMS (rTMS). *Ann Phys Rehabil Med*. 2015;58(4):208–213. doi:10.1016/j.rehab.2015.05.005
44. Zhai C, Wang Z, Cai J, et al. Repeated trans-spinal magnetic stimulation promotes microglial phagocytosis of myelin debris after spinal cord injury through LRP-1. *Exp Neurol*. 2024;379:114844. doi:10.1016/j.expneurol.2024.114844
45. Loy K, Bareyre FM. Rehabilitation following spinal cord injury: how animal models can help our understanding of exercise-induced neuroplasticity. *Neural Regen Res*. 2019;14(3):405–412. doi:10.4103/1673-5374.245951
46. Delarue Q, Robac A, Massardier R, Marie JP, Guérout N. Comparison of the effects of two therapeutic strategies based on olfactory ensheathing cell transplantation and repetitive magnetic stimulation after spinal cord injury in female mice. *J Neurosci Res*. 2021;99(7):1835–1849. doi:10.1002/jnr.24836